Serveur Académique Lausannois SERVAL serval.unil.ch

Author Manuscript
Faculty of Biology and Medicine Publication

This paper has been peer-reviewed but dos not include the final publisher proof-corrections or journal pagination.

Published in final edited form as:

Title: Beclin 1-independent autophagy contributes to apoptosis in cortical neurons.
Authors: Grishchuk Y, Ginet V, Truttmann AC, Clarke PG, Puyal J
Journal: Autophagy
Year: 2011 Oct
Volume: 7
Issue: 10
Pages: 1115-31
DOI: 10.4161/auto.7.10.16608

In the absence of a copyright statement, users should assume that standard copyright protection applies, unless the article contains an explicit statement to the contrary. In case of doubt, contact the journal publisher to verify the copyright status of an article.

serval
serveur académique lausannois

UNIL | Université de Lausanne
Faculté de biologie
et de médecine

Beclin1-independent autophagy contributes to apoptosis in cortical neurons

Yulia Grishchuk,[1]* Vanessa Ginet,[1,2]* Anita C. Truttmann,[2] Peter G.H. Clarke[1] and Julien Puyal[1]&

[1]Département de Biologie Cellulaire et de Morphologie, Université de Lausanne,

Rue du Bugnon 9, CH1005 Lausanne, Switzerland

[2] Division de Néonatologie, Département Médico-Chirurgical de Pédiatrie, Centre Hospitalier Universitaire Vaudois Lausanne, CH1011 Lausanne, Switzerland

*Equal Contributions

&To whom correspondence should be addressed:

JulienPierre.Puyal@unil.ch;

phone: +41 (0)21 692 5122; FAX: +41 (0)21 692 5255

Keywords: autophagy, apoptosis, neurons, cell death, lysosomes, caspases.

Acknowledgments: We thank Coralie Rummel, Florine Fonknechten and Vincent Mottier for technical assistance, and Jean-Yves Chatton and Yannick Krempp of the Cellular Imaging Facility (University of Lausanne) for experimental support. This research was supported by grants from the Swiss National Science Foundation (3100A0-113925 and 310030-130769), from the Fondation Motrice, from the Société Académique Vaudoise, from the Fondation Marie-Thérèse et René Planiol and from the Fondation Emma Muschamp.

Abbreviations: AcHex, β-N-acetylhexosaminidase; AIF, Apoptosis inducing factor; AP, acid phosphatase; ANOVA, analysis of variance; BA1, bafilomycin A1; LAMP1, lysosomal-associated membrane protein 1; LC3, microtubule-associated protein 1 light chain 3; 3-MA, 3-methyladenine; Q-VD-OPH, Quinoline-Val-Asp(ome)-Ch2-O-phenoxy; PI3K, phosphatidylinositol 3-kinase; STS, staurosporine.

Running title: Autophagy in neuronal apoptosis

Abstract

Neuronal autophagy is enhanced in many neurological conditions, such as cerebral ischemia and traumatic brain injury, but its role in the associated neuronal death is controversial, especially under conditions of apoptosis. We therefore investigated the role of autophagy in the apoptosis of primary cortical neurons treated with the widely used and potent pro-apoptotic agent, staurosporine (STS). Even before apoptosis, STS enhanced autophagic flux, as shown by increases in autophagosomal (LC3-II level, LC3 punctate labeling) and lysosomal (cathepsin D, LAMP1, acid phosphatase, β-hexasominidase) markers. Inhibition of autophagy by 3-methyladenine, or by lentivirally-delivered shRNAs against Atg5 and Atg7, strongly reduced the STS-induced activation of caspase-3 and nuclear translocation of AIF, and gave partial protection against neuronal death. Pan-caspase inhibition with Q-VD-OPH likewise protected partially against neuronal death, but failed to affect autophagy. Combined inhibition of both autophagy and caspases gave strong synergistic neuroprotection. The autophagy contributing to apoptosis was Beclin1-independent, as shown by the fact that Beclin1 knockdown failed to reduce it but efficiently reduced rapamycin-induced autophagy. Moreover the Beclin1 knockdown sensitized neurons to STS-induced apoptosis, indicating a cytoprotective role of Beclin1 in cortical neurons. Caspase-3 activation and pyknosis induced by two other pro-apoptotic stimuli, MK801 and etoposide, were likewise found to be associated with Beclin1-independent autophagy and reduced by the knockdown of Atg7 but not Beclin1. In conclusion, Beclin1-independent autophagy is an important contributor to both the caspase-dependent and –independent components of

neuronal apoptosis and may be considered as an important therapeutic target in neural conditions involving apoptosis.

Introduction

Enhanced autophagy has been implicated in various neurological conditions including cerebral ischemia and head injury,[1,2] but its role is controversial, and there is evidence that it can promote either cell survival or cell death according to the situation.[3,4]

Early arguments for a death-promoting role focused on morphological descriptions of dying cells during development, when autolysosomes can fill the cytoplasm and digest nuclear DNA.[5] Subsequent evidence in favor of this interpretation came from numerous reports that "autophagic cell death" (i.e. cell death manifesting intense autophagy) can be prevented by pharmacological prevention of autophagy[6-8] or by knockdown of autophagy genes.[9-12] On the basis of such evidence, most researchers accept that autophagy is a major mediator of cell death in a wide range of important situations,[13] including normal development and metamorphosis[5,14], AIDS[15], cerebral ischemia[1,2] and cancer therapy.[16] There is nevertheless controversy, and some opponents of this view minimize the role of autophagy in cell death.[17]

Nevertheless, a major remaining question is whether autophagy does so by a separate death effector mechanism independent of apoptosis, or whether it is a trigger for the latter or dependent upon it. There is evidence that both alternatives may be true depending on the situations.[13] In support of an independent death mechanism, autophagy has been shown in some cases to promote caspase-independent cell death[9,10,18] and an alternative death pathway in cells incompetent for apoptosis.[11,12] On the other hand, there is evidence that autophagic pathways can modulate caspase-mediated apoptosis.[2,19-21] Furthermore, it is now well demonstrated that autophagy and apoptosis can share common regulators.[4,13,22]

It is therefore important to clarify the relationship between autophagy and apoptosis as a prelude to neuroprotection by interfering with autophagy.[1,2,20,23,24] We therefore here

investigate the role of autophagy in neuronal apoptosis caused by classical apoptotic stimuli, especially the protein kinase inhibitor staurosporine.[25,26]

Results

A strong autophagosomal increase precedes STS-induced apoptosis in cortical neurons

Staurosporine (STS), a classical apoptotic stimulus that has been previously widely characterized to induce apoptosis in several different cell types including primary neuronal cultures,[25-27] was used to promote apoptosis in primary cultures of cortical neurons. In the present experiments, 1μM STS induced neuronal death as demonstrated by a progressive increase in the number of pyknotic nuclei from 6h of STS treatment **(Fig. 1a)** or in lactate dehydrogenase (LDH) release into the medium (**Suppl. fig. 1a**)**.** As expected, STS gradually but strongly increased caspase-3 activation as shown by immunoblotting for cleaved caspase-3 (**Fig. 1b, Suppl. fig. 1b**), and also for α-fodrin, which showed an increase in the 120kDa caspase-dependent cleavage fragment from 6h of STS (**Suppl. fig. 1c**). Moreover the 145/150kDa calpain-dependent cleavage fragment of α-fodrin likewise increased, indicating progressive calpain activation (**Suppl. fig. 1c**).

Interestingly, along with the induction of caspase-3 and calpains, STS-treated neurons showed raised levels of autophagosomal marker LC3-II. LC3-II detected by immunoblotting was increased as early as 30min after STS exposure, reaching the maximum value at about 12h and decreasing by 24h, suggesting a substantial increase in autophagosome formation after STS treatment (**Fig. 1b, Suppl. fig. 1b**). Together, the pattern of cleaved caspase-3 and LC3-II expressions indicates that autophagosome enhancement (30min-12h) is followed by a progressive activation of caspase-3 (1h-24h). Additionally, an increase in autophagosome formation over the time was demonstrated by time-lapse imaging in neurons overexpressing Sapphire-LC3 (**Suppl. fig. 1d**) or by counting the number of LC3-positive dots per mm^2 and

per neuron following immunolabeling against LC3 **(Fig. 1c)**. Both results show a strong and gradual increase in LC3 positive vesicular structures as early as 3h after STS.

Lysosomal activation and autophagic flux are induced in STS-induced neuronal apoptosis

To demonstrate that STS-induced autophagosome increase was caused by activation of the autophagy/lysosomal pathway and was not a result of impaired downstream autophagosome fusion and degradation by lysosomes, we investigated the effect of STS on lysosomal activity. An enzymatic assay for acid phosphatase (AP) was performed on protein extracts of cortical neurons treated with STS for different times (**Fig. 2a**). AP activity was moderately increased after 3h and 6h of STS compared to the basal activity of control neurons, but then returned to control levels at 12h and 24h. But in contrast to this minor change in the total AP activity, we found by AP histochemistry a most striking change in the distribution of the activity, which appeared in a greater number of large puncta in the 6h STS-treated neurons, as shown in **figure 2b**. In fact, the percentage of small puncta ($\leq 0.3 \mu m^2$) per neuron was not affected, but there was a switch from intermediate- (>0.3 and $\leq 0.9 \mu m^2$) to large- ($>0.9\ \mu m^2$) size puncta in STS-treated neurons, reflecting putatively the creation of autolysosomes by the fusion of autophagosomes with lysosomes. Cytochemical staining for another lysosomal enzyme, β-N-acetylhexosaminidase (AcHex), was also performed and clearly showed a strong increase in AcHex activity in larger puncta following 6h of STS compared to control neurons (**Fig. 2c**). Immunocytochemical staining for two lysosomal markers, lysosomal-associated membrane protein 1 (Lamp1) and the lysosomal protease cathepsin D, confirmed the enlargement of lysosomes 6h after STS exposure (**Suppl. fig. 1e**). Double

immunolabeling for Lamp1 and LC3 showed LC3-positive puncta (autophagosomes) and enlarged lysosomes within the same neurons (**Suppl. fig 1f**).

We investigated then the expression of p62/SQSTM1, a long-lived protein known to be selectively degraded by autophagy.[28] Addition of STS induced a progressive and strong reduction in p62/SQSTM1 suggesting an increase in the whole process of autophagy **(Fig. 2d)**. To further confirm that the STS-induced autophagosome increase was due to autophagy induction and not impaired autophagosome-lysosome fusion, we used bafilomycin A1 (BA1), a vacuolar type H^+-ATPase inhibitor that prevents lysosome acidification and autophagosome-lysosomal fusion. Treatment for 12h with BA1 (300nM), at which concentration autophagosome-lysosomal fusion is completely blocked, led as expected to a substantial accumulation of autophagosomes (LC3-II level) and of p62/SQSTM1 (**Fig. 2e**). Importantly, when this 12h BA1 treatment was combined for the last 6h with STS this resulted in a greater increase in the LC3-II level than with BA1 or STS alone and in the prevention of p62 degradation normally induced by STS (**Fig. 2e**). To evaluate whether the increase in autophagosome formation induced by STS also led to maturation into autolysosomes, we used an RFP-GFP-LC3 DNA construct in order to discriminate between early and late autophagosomes (**Fig. 2f**). Following STS treatment, besides confirming a global increase in the total number of autophagosomes, STS increased both the number of early autophagosomes (GFP^+ RFP^+ LC3-positive dots) and the number of late autophagosomes (GFP^- RFP^+ LC3-positive dots) demonstrating that the maturation of autophagosomes into autolysosomes is also increased upon STS treatment. Taken together, these results confirm that STS-induces *de novo* formation of autophagosomes and enhanced autophagic flux.

Activation of lysosomes and caspase-3 in the same neuron

Double immunolabeling for Lamp1 and cleaved caspase-3 revealed that neurons displaying condensed chromatin were always positive for cleaved caspase-3 and that some of them were also characterized by enhanced Lamp1 labeling 12h after STS treatment (**Suppl. fig. 1g**). Since neurons with non-condensed chromatin also often presented strong Lamp1 staining but were negative for cleaved caspase-3, and since some with condensed chromatin were only very weakly positive for Lamp1, these observations confirm our Western blot results (**Fig. 1b, Suppl. fig. 1b**) suggesting that enhanced autophagy precedes caspase-dependent apoptosis and that Lamp1 staining dissipates as apoptosis progresses.

Mitophagy is not involved in STS-induced neuronal apoptosis

Since, in some conditions, autophagy can inhibit apoptosis by removing dysfunctional mitochondria or aggravate it by an excessive destruction of mitochondria, we tested if STS induced mitophagy. We examined whether the mitochondrial marker mtHSP70 colocalized with autophagosome/lysosome markers. Double-immunofluorescent analysis revealed very few colocalizations of mtHSP70, either with autophagosomes (dots of LC3 staining) or with the lysosomal marker cathepsin B (**Suppl. fig. 2a, b**).

Pharmacological inhibition of autophagy and caspases are both protective but more efficient when combined

To further investigate the role of enhanced autophagy in STS-induced neuron death, we investigated the effects of 3-methyladenine (3-MA), a widely used autophagy inhibitor, and

of a broad spectrum caspase inhibitor, Q-VD-OPH. Pre-treatment with 3-MA (10mM) resulted in a significant neuronal protection as measured by counts of pyknotic nuclei (**Fig. 3a**) or by the LDH release assay (**Suppl. fig. 3a**) 12h after exposure to STS. Pre-treatment with Q-VD-OPH (25μM) resulted in a better protection than with 3-MA, and combination of both inhibitors was more efficient than either alone since neuronal death was almost totally prevented (**Fig. 3a, Suppl. fig. 3a**).

Pre-treatment with Q-VD-OPH completely prevented caspase-3 activation as shown by immunoblot for cleaved caspase-3 (**Fig. 3b**) and for caspase-dependent α-fodrin cleavage (**Suppl. fig. 3d**), without any effect on the LC3-II level (**Suppl. fig. 3c**) or on calpain activation (**Suppl. fig. 3d**). In addition to decreasing autophagy (**Suppl. fig. 3b**), 3-MA treatment significantly reduced caspase-3 activation (shown by decreases in both cleaved caspase-3 (**Fig. 3b**) and caspase-3-mediated α-fodrin cleavage (**Suppl. fig. 3d**)), as well as calpain activation (shown by the reduction in calpain-mediated α-fodrin cleavage (**Suppl. fig. 3d**)). We evaluated also the effect of 3-MA on caspase-independent apoptosis by investigating apoptosis inducing factor (AIF) translocation to the nucleus after STS treatment. 3-MA strongly reduced the AIF translocation normally induced 6h after STS treatment (**Fig. 4d**) whereas Q-VD-OPH as no effect on it (not shown). The strong neuroprotective effect of 3-MA and Q-VD-OPH in combination was reflected in a robust decrease in both apoptosis (caspases and AIF) and calpains (**Fig. 3b, Suppl. fig. 3d**).

Knockdown of Atg5 or Atg7 reduces STS-induced neuronal apoptosis and is strongly protective when combined with caspases inhibition

In view of the possible non-specific effects of 3-MA in addition to the inhibition of autophagy, we performed a knockdown of different autophagy genes with lentiviral vectors encoding short hairpin RNAs (shRNAs): Atg5, Atg7 and Beclin1/Atg6.

Atg5 knockdown was confirmed by Q-RT-PCR, which showed that Atg5 mRNA expression in shRNA-Atg5 transduced neurons was inhibited by 55% (**Fig. 4a**). Downregulation of Atg5 decreased autophagosome formation in response to STS treatment as shown by a decrease in punctate Sapphire-LC3 (**Fig. 4b**) and by a reduction of about 30% in LC3-II level after STS exposure (**Fig. 4c**). Atg5 knockdown resulted also in decreased activation of caspase-3, as shown in Western blots by reduced immunoreactivity of both cleaved caspase-3 (**Fig. 4d**) and caspase-specific α-fodrin fragment (**Suppl. fig. 4a**). Downregulation of Atg5 decreased significantly the number of pyknotic nuclei (**Fig. 4e**) or release of LDH (**Suppl. Fig. 4d**) than control-infected neurons 12h after STS treatment, implying a higher survival rate. Moreover, pre-treatment of cultures with Q-VD-OPH had a strong protective effect when combined with Atg5 knockdown, reducing both the percentage of pyknotic neurons (**Fig. 4e**) and the release of LDH (**Suppl. Fig. 4d**). This synergistic neuroprotective effect indicates that caspase-independent autophagy-related mechanisms are involved in the execution of STS-induced neuron death. Similar results were obtained with the combination of two Atg7 shRNAs which gave a very strong inhibition of Atg7 expression as shown by Q-RT-PCR (**Fig. 5a**) or by Western blot (**Fig. 5b**). Neurons transduced with Atg7 shRNAs showed not only a strongly decreased STS-induced autophagosome formation as demonstrated by a decrease in Sapphire-LC3 positive dots (**Fig. 5c**) and in LC3-II level (around 58%) by immunoblots (**Fig. 5d**), but also inhibition of caspase-3 (**Fig. 5e** and **Suppl. fig. 4b**) and calpain (**Suppl. fig. 4b**). Cell death quantification demonstrated strong reduced

toxicity in Atg7 knockdown neurons as shown by decrease in pyknotic nuclei 12h after STS (**Fig. 5f**) and by measurement of LDH-release (**Suppl. Fig. 4e**). Moreover knockdown of Atg5 or Atg7 strongly prevented STS-induced intra-nuclear AIF accumulation as shown in **figure 6**. These results suggest that autophagy plays a role upstream of apoptosis.

To confirm a death promoting role of excessive autophagy following STS, we investigated whether the upregulation of Atg7 gave opposite results to Atg7 downregulation **(Fig. 7)**. Neurons transduced with Atg7-myc lentiviral vector, which strongly overexpressed Atg7 (**Fig. 7a**), displayed enhanced autophagosome formation as shown by an increase in LC3 positive puncta following immunolabeling (**Fig. 7b**) or by LC3-II level in Western blot analysis (**Fig. 7c**). Moreover, this effect was enhanced in the presence of STS and Atg7 upregulation sensitized the neurons to STS-induced apoptosis since both the level of cleaved caspase-3 (**Fig. 7c**) and the number of pyknotic nuclei (**Fig. 7e**) were markedly increased; even in the absence of STS there was a moderate induction of apoptosis when Atg7 was overexpressed (**Fig. 7c,e**). The sensitization to STS induced by Atg7 overexpression could be prevented by the addition of 3-MA or by Atg5 knockdown (**Suppl. Fig. 6**).

Taken together, the data from the Atg5 and Atg7 knockdown experiments are similar to those obtained with the pharmacological inhibition of autophagy, and demonstrate an involvement of autophagy in the mediation of STS-induced neuronal apoptosis through both caspase-dependent and independent pathways.

Autophagy enhanced in STS-induced neuronal apoptosis is Beclin1-independent but Beclin1 knockdown sensitizes neurons to caspase-dependent apoptosis

It has been shown that Beclin1 can be involved in autophagic cell death following some stimuli.[12,29] Surprisingly, strong downregulation of Beclin1 (by 75%) (**Fig. 8a**) did not affect STS-induced autophagosome formation (**Fig 8b, c**), whereas it strongly inhibited autophagosome formation induced by rapamycin (**Fig. 8d**) as expected[30] or in basal conditions (**Suppl. Fig 7c**). These results indicate that while Beclin1 is involved in the regulation of the mammalian Target of Rapamycin (m-TOR) dependent autophagic pathway in neurons, STS-induced autophagy is Beclin1-independent.

We observed that Beclin1 knockdown was accompanied by a strong activation of caspase-3 (compare to the control infected neurons) in the presence and even in the absence of STS (**Fig. 8e** and **Suppl. fig. 4c)**, thus sensitizing neurons to death (increase in pyknotic nuclei and LDH-release (**Fig. 8f and Suppl. fig. 4f**)). Q-VD-OPH treatment very efficiently reduced STS-induced toxicity in neurons transduced with Beclin1 shRNA (**Fig. 8f**). Downregulation of Beclin1 in STS-treated neurons also caused a 2.6-fold stronger activation of calpain compared to control-infected neurons, as shown by an increase in calpain-dependent cleavage of α-fodrin (**Suppl. fig. 4c**).

Overexpression of Beclin1 did not result in any significant effects on the STS-induced apoptosis and autophagy (neurotoxicity, LC3-II accumulation, caspase and calpain activation) (**Suppl. fig. 5**) confirming that Beclin1 is not involved in STS-induced neuronal death.

Similar role of Beclin1-independent autophagy in apoptosis caused by other stimuli

To evaluate whether our results can be generalized beyond apoptosis induced by STS, we investigated the role of autophagy in neuronal death due to two other frequently used

apoptotic stimuli, MK801 (40μM) and etoposide (10 μM).[31-33] Both stimuli led not only to an increase in cleaved caspase-3, but also in LC3-II level (**Fig. 9a, b**) and LC3-positive puncta (**Suppl. Fig. 8a, b**) suggesting an induction of autophagy, which was moreover independent of Beclin1 (**Suppl. Fig. 8c, d**) but Atg7-dependent. Atg7 downregulation prevented the increases in both LC3-II and cleaved caspase-3 following 48h of treatment with MK801 (**Fig. 9c**) or etoposide (**Fig. 9d**) and provided neuroprotection as shown by a reduction in the numbers pyknotic nuclei (**Fig. 9e, f**). In contrast, Beclin1 downregulation, increased the activation of caspase-3 following treatment with MK801 or etoposide and increased the numbers of pyknotic nuclei (**Suppl. Fig. 8c, d**).

The latter results indicate that the autophagic control of apoptosis occurs with other apoptotic stimulations than STS, and may be considered an important contributor to the neuronal apoptotic response.

Discussion

The present study shows that, following apoptotic stimulation in cortical neurons, autophagy is strongly enhanced and involved in mediating both the caspase-dependent and -independent components of the apoptosis. Moreover this induced autophagy is dependent on autophagy genes Atg5 and Atg7 but is Beclin1-independent, suggesting that a selective and noncanonical pathway of autophagy contributes to neuronal apoptosis.

Staurosporine induces autophagy prior to caspase activation

Our observations on caspase-3 and AIF release and protection by caspase-inhibition agree with previous studies on STS-treated on cortical neurons.[25,26] Only a few studies have reported STS-induced autophagy in unmodified cells[34,35] especially in cortical neurons,[36] but in specific conditions, such as in fibroblast mutants incompetent for apoptosis, STS has been reported to cause autophagic cell death that is blocked by 3-MA or by knockdown of Atg5 or Beclin1.[11] Also, in cell lines exposed to a caspase inhibitor, STS promoted a rapid activation of autophagy prior to apoptosis.[37] In the present study we showed not only an early increase in autophagosome formation following STS exposure of cortical neurons but also an activation of the lysosomal pathway, thereby demonstrating an increase in autophagic flux. Moreover autophagy, lysosomal activation (acid phosphatase, β-hexasominidase, cathepsin D) and apoptosis occurred in the same neurons, although enhanced autophagic and lysosomal features appeared earlier than caspase-3 activation, suggesting that autophagy might be involved in triggering apoptosis.

Induced autophagy contributes to neuronal apoptosis

To test this possibility we needed to inhibit autophagy. The only available pharmacological inhibitors of autophagy are PI3-K inhibitors, of which the most frequently used for studies of autophagy is 3-MA, although wortmannin and LY294002 are also used.[6,7,11] These inhibitors reduce autophagy by virtue of their action on class III PI3-K, but they also affect the other classes of PI3-K including class I, which activates the powerfully anti-apoptotic and anti-autophagic Akt pathway. Therefore, even if these pharmacological inhibitors were rigorously specific for PI3-Ks, which is not the case,[38] they would still not be specific inhibitors of autophagy. In the present study we used 3-MA, which is in many cases a very effective inhibitor of autophagy, but not always because, by virtue of its inhibition of class I PI3-K, it can even promote autophagy, especially after long exposure.[39] This may help to explain why the autophagy inhibition by 3-MA was only partial in the present experiments, but the Beclin1-independence of the autophagy may also be relevant, because class III PI3-K interacts with Beclin1 and the role of class III PI3-K in Beclin1-independent autophagy is currently unclear. In view of these limitations of 3-MA as an autophagy inhibitor, it is important that our shRNA-mediated downregulation of Atg5 and Atg7 gave similar results to pharmacological inhibition with 3-MA. All these three ways of inhibiting autophagy decreased neuronal apoptotic features and death, and they all strongly enhanced the protection in neurons exposed to Q-VD-OPH.

It is now clear that autophagy and apoptosis share several common effectors such as PUMA/Bax,[40] FLIP proteins[41] or Atg4D.[42] Enhanced autophagy can prevent[43] or activate[8,19,44] apoptosis depending on the conditions. Two studies showed that Atg5 could promote apoptosis induction independently of its role in autophagy. Atg5 interacted with Fas-associated protein with death domain and stimulated caspase-dependent cell death in

HeLa cells treated with IFNγ.[45] Moreover, in response to several apoptotic stimuli Atg5 has been shown to be cleaved by calpain, following which a cleavage fragment translocates from the cytosol to mitochondria triggering cytochrome c release and caspase activation.[21] In the present study, however, calpain-mediated effects seem not to be the cause of caspase activation because treatment with the calpain inhibitor ALLN increased caspase-3 activation rather than reducing it (data not shown). We cannot strictly rule out contributions from other autophagy-independent mechanisms, but the similar reductions of apoptotic features obtained with three different means of autophagy inhibition, 3-MA treatment and Atg7 knockdown as well as Atg5 knockdown, suggest that the autophagic pathway was involved. Furthermore, we have also shown that overexpression of Atg7 leads to increased autophagy and apoptosis even in the absence of an apoptotic agent. Moreover blockade of autophagy by Atg5 knockdown prevents this sensitization induced by Atg7 overexpression, demonstrating that the pro-death effects of Atg7 overexpression are mainly autophagy-dependent.

Although most of our experiments involved STS-induced autophagy, we tested other apoptotic stimulations to confirm the generality of the phenomena. Using MK801 and etoposide we again demonstrated the efficacy of Atg7 knockdown for reducing caspase-3 activation and nuclei pyknosis. Thus, our conclusions are relevant to other apoptotic stimulations than STS, suggesting that autophagy, or autophagic signalling, is an important inducer of neuronal apoptosis in multiple situations.

The autophagy-apoptosis link does not depend on Beclin1

Another important link between apoptosis and autophagy is the interaction between Bcl2 and Beclin1, because Bcl2 is both anti-apoptotic and anti-autophagic. Beclin1 was first identified

as a protein binding to Bcl2 through its BH3 domain. In basal conditions Beclin1 is sequestered by Bcl2 and under stress conditions Beclin1 is released and induces autophagy.[46] However, although Bcl2 has a strong anti-autophagic effect, overexpression of Beclin1 did not affect apoptosis[47] as observed also in the present study. Thus, although Beclin1 might theoretically be pro-apoptotic by sequestering Bcl2 and thereby counteracting its anti-apoptotic action, it is apparently not sufficiently abundant to actually do so in the present experiments. Furthermore, our results concerning Beclin1 downregulation are the very opposite of what might be predicted from its sequestering of Bcl2, because the downregulation strongly induced neuronal apoptosis in basal conditions as well as sensitizing neurons to STS-induced apoptosis. Our observations thus suggest an essential role of Beclin 1 for neuronal survival in basal and STS conditions, and similar results with Beclin1 downregulation have been suggested previously in different models.[43,48]

Some recent observations on the death of differentiated neural precursor cells resemble ours to the extent that the cell death was reduced by the knockdown of Atg7 but not Beclin1.[49] However, the experimental model was very different from ours, involving treatment with chloroquine or bafilomycin A1, both of which reduce autophagic flux, either by inhibiting lysosomal functions (chloroquine) or by blocking the fusion of autophagosomes to lysosomes (bafilomycin A1). This contrasts with our experiments in which STS induced an *increase* in autophagic flux in cortical neurons including an enhanced lysosomal degradative activity, so the relationship between the two experimental situations is unclear.

Induced-autophagy in neuronal apoptosis is Beclin1-independent

Beclin1 is an important autophagy regulator playing several different roles along the autophagic process. Beclin1 can act in the induction step prior to autophagy,[49,50] in autophagosome formation[51] and in autophagosome maturation.[50] Our experiments with Beclin1 knockdown showed that, although a ~75% reduction in Beclin1 protein efficiently reduced rapamycin-induced autophagy, it did not affect autophagosome formation after exposure to STS, indicating that STS triggers a Beclin1-independent autophagy in dying cortical neurons. We have similar evidence for Beclin1-independent autophagy following MK801 and etoposide treatments, supporting the generality of the phenomenon. Beclin1-independent autophagy has been reported in only a few previous cases. In SH-SY5Y cells exposure to the neurotoxin 1-methyl-4-phenylpyridinium (MPP+) provoked autophagy and cell death that were insensitive to PI3-K inhibition or Beclin1 knockdown.[52,53] Likewise, autophagy that is insensitive to knockdown of Beclin1 or of its binding partner hVps34 (i.e. class III PI3-K) is involved in the caspase-independent death of cancer cells induced by resveratrol,[54] in the hydrogen peroxide induced death of GSH-depleted RAW 264.7 cells,[55] in the obatoclax-induced death of various cancer cells[56] and in HeLa cells treated with an inhibitor of the the BH3-binding groove of Bcl-XL/Bcl-2.[57]

Increased expression of Beclin1 has sometimes been considered a marker of enhanced autophagy in neurons in various neurodegenerative conditions including closed head injury, traumatic brain injury, spinal cord injury and focal cerebral ischemia.[58-60] The existence of Beclin1-independent autophagic mechanisms emphasizes the limitations of Beclin1 as an autophagy marker.

The reason for the lack of effect of Beclin1 knockdown on autophagy and neuronal death is unknown, but a contributing factor may be the disactivation of Beclin1 by caspase-

mediated cleavage, which occurs in cell lines exposed to various apoptotic stimuli including STS.[61] We do in fact have evidence that Beclin1 was cleaved in our neurons exposed to STS for 12h and that this cleavage was caspase-dependent (**Suppl. Fig. 9**). The amount of full-length Beclin1 was only moderately decreased, however, so Beclin1 depletion would only partially explain the lack of effect of Beclin1 knockdown, and would not at all explain their sensitization to STS-induced apoptosis.

In conclusion, our study highlights the importance of checking for autophagy involvement when apoptosis is induced. It shows with three different apoptotic stimuli that Beclin1-independent Atg5/Atg7-dependent autophagy (or at least autophagic signalling) is an important inducer of both the caspase-dependent and –independent components of neuronal apoptosis. The long term prospect of being able to inhibit both components by inhibiting only one selective pathway of autophagy opens new avenues for clinically useful neuroprotection.

Materials and Methods

Lentiviral vectors and virus production. CDNAs encoding full-length rat Atg7 (GenBank™ NM_001012097) and Beclin-1 (GenBank™ NM_053739) with C-terminal Myc-tag was created using PCR with specific primers (Atg7: nucleotides 16-35 (forward), 2092-2112 (reverse); Beclin-1: nucleotides 225-243 (forward), 1549-1570 (reverse)) to which the myc-tag encoding sequence was added. Resultant cDNAs and rat MAP LC3B (GenBank™ NM_022867) cDNA fused to the C-terminus of Sapphire fluorescent protein cDNA (a generous gift of Dr. Shibata and Prof. Uchiyama) were cloned into a self-inactivating lentiviral transfer vector under the control of mouse phosphoglycerate kinase 1 (PGK) promoter (SIN-W-PGK)[61] using the pENTR/D-TOPO cloning Kit (Invitrogen, Carlsbad, CA, USA) and the LR recombination reaction (Gateway system, Invitrogen). shRNAs specific for rat genes from TRC (the RNAi consortium) library in pLKO lentiviral vectors were used as follows: TRCN0000099431 for ATG5 (GenBank™ NM_001014250.1), TRCN0000033552 for Beclin1 (GenBank™ NM_053739.2), and a combination of TRCN0000092163 and TRCN0000092166 for ATG7 (GenBank™ NM_001012097) (Openbiosystems). Self-inactivating lentiviral vectors were produced as described previously.[63]

Primary cortical neuronal cultures. All experiments were performed in accordance with the Swiss Law for the protection of animals and were approved by the Vaud Cantonal Veterinary Office. Primary neuronal cultures were prepared from the cortices of 2-day-old Sprague-Dawley rats (from Janvier, France) and maintained as described previously.[64] For biochemical analyses and LDH release measurement, neurons were plated at a density of

$6x10^5$ cells/dish (35mm poly-D-lysine precoated dishes, BD Biosciences, 356467). For immunocytochemistry, neurons were plated at a density of $1.5x10^4$ cells/well of 24 well plates (or $9.6x10^4$ cells/well for lentiviral infection experiments) on 12mm coverslips coated with 0.01% poly-L-lysine (Sigma, P4832). Cells were maintained at 37°C with a 5% CO_2-containing atmosphere for 12 days, and half of the media was changed every 3-4 days.

For lentiviral-mediated protein expression and knockdown, cultures were infected on day in vitro (DIV) 7 using 50ng of p24/ml culture medium for each vector, and half the medium was replaced on DIV 11. Empty vectors were used as an infection control. Control infection did not cause any strong effect on LDH release, or on the expression of autophagy marker LC3-II, or cell death markers (cleaved caspase-3 or calpain or caspase-3 specific α-fodrin cleavage fragments) compared to non-infected neurons after staurosporine treatment (**Supplementary table 1**).

Pharmacological treatment. At DIV 11-12 primary cortical neurons were exposed to 1μM staurosporine (STS) (Sigma-Aldrich, S4400) or 0.1% DMSO (Sigma-Aldrich, 154938) in complete culture medium for indicated times. Where specified, cells were pre-treated for 1h prior to STS application with 25μM of the pan-caspase inhibitor Q-VD-OPH (Quinoline-Val-Asp(ome)-Ch2-O-phenoxy; MP Biomedicals, 030PH10903) or 10mM of the autophagy inhibitor 3-methyladenine (3-MA) (Sigma-Aldrich, M9281). Bafilomycin A1 (Enzo Life Sciences, ALX-380-030-M001) was applied for 6h prior to STS. For the other treatments, primary cortical neurons were incubated with 10μg/ml rapamycin (Sigma, R0395) for 24h, with 40μM MK801 (Sigma-Aldrich, M107) or 10μM etoposide (Sigma-Aldrich, E1383) for 24h and 48h.

Immunoblotting. Protein samples were harvested in lysis buffer (20 mmol/L HEPES, pH 7.4, 10 mmol/L NaCl, 3 mmol/L $MgCl_2$, 2.5 mmol/L EGTA, 0.1 mmol/L dithiothreitol, 50 mmol/L NaF, 1 mmol/L Na_3VO_4, 1% Triton X-100 (reagents from Sigma-Aldrich), and a protease inhibitor cocktail (Roche, 11873580001)). Lysates were sonicated and protein concentration was determined using a Bradford assay. Proteins (20-40μg) were separated by SDS-PAGE on a 10% or 14% polyacrylamide gel, and analyzed by immunoblotting. The following primary antibodies were used for protein immunodetection: anti APG7 (sc-33211, 1/1000) rabbit polyclonal, anti-Beclin1 (sc-11427, 1/1000) and anti-α-tubulin (sc-8035, 1/5000) mouse monoclonal antibodies from Santa Cruz Biotechnology (Santa Cruz, CA, USA); anti-LC3 (ab48394, 1/3000) rabbit polyclonal antibody from Abcam (Cambridge, UK); anti-active caspase-3 (#9661, 1/1000) and anti-AIF (#4642, 1/1000) rabbit polyclonal antibodies from Cell Signalling Technology (Danvers, MA, USA); anti p62/SQSTM1 (P0067, 1/1000) rabbit polyclonal antibody from Sigma-Aldrich and anti-fodrin (#FG6090, 1/3000) mouse monoclonal antibody from Biomol (Enzo Life Sciences, Lausen, Switzerland). After incubation with primary antibody, the following secondary antibodies were applied: polyclonal goat anti-mouse or goat anti-rabbit IgG conjugated with IRDye 680 (LI-COR, B70920-02) or IRDye 800 (LI-COR, 926-32210). Protein bands were visualized using the Odyssey Infrared Imaging System (LI-COR). Odyssey v1.2 software (LI-COR) was used for densitometric analysis. OD values were normalized with respect to tubulin and expressed as a percentage of values obtained for non-infected neurons treated with 0.1% DMSO (100%). All data were expressed as mean ± SEM. Data were analyzed statistically by

one-way ANOVA followed by Student's t-test (two-tailed, two-sample, and unequal variance).

Immunocytochemistry. Primary cortical neurons cultured on glass coverslips were fixed with 4% paraformaldehyde in PBS (pH 7.4) for 15min on ice, and incubated for blocking and permeabilization in PBS with 10% donkey serum and 0.1% Triton X-100 for 1h. Cells were incubated with primary antibodies diluted in 5% of donkey serum, 0.1% Triton X-100 in PBS overnight at 4°C. The following primary antibodies were used: anti-mtHSP70 (ma3-028, 1/100) mouse monoclonal antibody from ABR (Affinity Bioreagents, Golden, CO, USA); anti-cathepsin B (#06-480, 1/200) and anti-cathepsin D (#06-467, 1/200) rabbit polyclonal antibody from Upstate Biotechnology (Lake Placid, NY); anti-NeuN (#MAB377, 1/500) mouse monoclonal antibody from Chemicon, (Temecula, CA, USA); anti-GFP (#AB3080, 1/500) rabbit polyclonal antibody and anti-AIF rabbit polyclonal antibody (#AB16501; 1/200) from Millipore (Billerica, MA, USA). Anti-LC3 was a generous gift from Prof. Yasuo Uchiyama (Tokyo, Japan). Alexa Fluor 488 donkey-anti-rabbit (Invitrogen, A21206) and Alexa Fluor 594 donkey-anti-mouse (Invitrogen, A21203) secondary antibodies, diluted in PBS with 1% of donkey serum (1/1000), were applied for 2h at room temperature. Coverslips were mounted with FluoroSave (Calbiochem, 345-789-20) and analyzed with either Leica SP5 AOBS or Zeiss LSM 510 Meta confocal laser-scanning microscopes. Images were then processed by with Adobe Photoshop 5.0.

Plasmid transfection. Cells on 12mm coverslips were transfected using Lipofectamine 2000 (Invitrogen, 11668-019) as described previously.[65]

Time-lapse microscopy. Cortical neurons were plated onto poly-L-lysine-coated glass coverslips that had previously been attached with hot vaseline/wax (50:50) to 35mm plastic culture dishes in which holes 15mm in diameter had been machine drilled.[64] On DIV 12, dishes were placed on the stage of a Nikon TE300 microscope. Temperature was maintained at 37°C and CO_2 at 5% using a microscope incubator system (Solent Scientific Limited, UK). Selected neurons were imaged with a 40x objective at 5 min intervals. Images were captured with an Orca-ER cooled CCD camera (Hamamatsu). All peripherals were controlled with Metamorph software (Universal Imaging). Images were processed with either Adobe Photoshop or Metamorph.

Cytochemistry for lysosomal enzymes. DIV 12 cortical neurons plated on coverslips were washed and fixed at different times after STS treatment in 2% glutaraldehyde and 1% paraformaldehyde diluted in cacodylate buffer (0.1M, pH 7.4), washed three times in 0.1M cacodylate buffer (pH 7.3) and stained as previously described.[2] For acid phosphatase histochemistry coverslips were incubated for 2h at 37°C in 0.01M Na-β-glycerophosphate and 8μM lead nitrate in sodium acetate buffer (50mM, pH 5), rinsed in distilled water and immersed in ammonium sulphide (0.5%) for 30s, rinsed again and mounted with FluoroSave. Controls were performed using sodium fluoride (1M) to verify the labeling specificity. No staining was detected in any of these controls.

For β-N-acetylhexosaminidase cytochemistry coverslips were incubated for 1h at 37°C in Fast Red Violet salt solution (0.63M ethylene glycol monomethyl ether, 1% polyvinyl pyrrolidone, 0.1M citric acid-citrate buffer pH 4.4, 1.6M sodium chloride, 2.7mM

Fast Red Violet LB salt (Sigma, F3381)) using 0.5mM Naphthol-AS-BI-N-acetyl-β-D-glucosaminide (Sigma, N4006) as the substrate, post-fixed for 10 min. in 10% formaldehyde, dehydrated in graded alcohols and mounted in Eukitt medium. Controls without the substrate or at basic pH gave no staining. Image acquisition was performed with an Axiovision Zeiss microscope. Quantification of lysosomal enzyme staining was performed using Image J software and images were then processed with Adobe Photoshop 5.0.

Enzyme assay for acid phosphatase. Protein samples were prepared in the same lysis buffer as for immunoblotting but without NaF and Na_3VO_4, as previously described.[23] 10 μg of proteins diluted in sodium acetate buffer (0.1M, pH=5.5) with 20mM PNPP (p-Nitrophenyl Phosphate) was incubated for 2h at 37°C in a final volume of 400μl. The reaction was stopped by the addition of 50μl 2mol/L NaOH and absorbance was measured at 405nm.

Quantitative real-time PCR analysis. RNA was isolated by RNAeasy kit (Qiagen, 74106) using the manufacturer's instructions. For cDNA synthesis the High capacity cDNA Reverse Transcription kit was used (Applied Biosystems). Samples were analysed using Tagman expression assays for beta-actin, Rn00667869_m1; Atg5, Rn01767063_m1; Atg7, Rn01492725_m1. Gene expression was measured from 5 biological repeats and technical triplicates amplified on a 7900HT Real-Time PCR System with SDS 2.3 software (Applied Biosystems). Relative expression values (V) were calculated by the ΔCt method and normalyzed to beta-actin expression as previously described.[66]

Quantification of cell death. Cytotoxicity was calculated by measurements of lactate dehydrogenase (LDH) release in the medium by using the CytoTox 96 Non-Radioactive Cytotoxicity Assay (Promega, G1780) as previously described.[64] Data are expressed as a percentage of the LDH value of non-infected neurons treated with 0.1% of DMSO. Neuronal death was also evaluated by counting DAPI-stained pyknotic nuclei. Cells were examined using a Zeiss Axioplan 2 imaging microscope. Total number and pyknotic-positive nuclei were then counted using ImageJ software. Results were expressed as a percentage of pyknotic nuclei (relative to the total number of nuclei). Data were expressed as mean ± SEM and analyzed statistically by one-way ANOVA followed by Student's t-test (two-tailed, two-sample, and unequal variance).

Quantification of AIF nuclear translocation. AIF nuclear staining was examined using a Zeiss Axioplan 2 imaging microscope. Measures of AIF nuclear fluorescence were performed using ImageJ software and a 60x magnification objective and then expressed as an average of fluorescence intensity/μm^2. All data were expressed as mean ± SEM and analyzed statistically by one-way ANOVA followed by Student's t-test (two-tailed, two-sample, and unequal variance).

Quantification of LC3, Cathepsin B and mtHSP70 labelling. Confocal images of immunocytochemistry against LC3, cathepsinB and mtHSP70 or of transfected neurons with mRFP-GFP-LC3 DNA construct on coverslips of cortical neuronal cultures at different time points after STS treatment (0, 3, 6, 12 and 24h) were acquired using a Zeiss LSM 710 Meta confocal laser-scanning microscope. LC3, cathepsinB and mtHSP70 positive dots were then

analysed using ImageJ software and expressed as a number of positive dots per neuron. All data were expressed as mean ± SEM and analyzed statistically by one-way ANOVA followed by Student's t-test (two-tailed, two-sample, and unequal variance).

Statistical analysis. Data represent the mean values ± SEM. Data were analyzed statistically by one-way ANOVA followed by Students' t-test (two-tailed, two-sample, and unequal variance) when ANOVA showed significant differences between the groups ($p<0.05$). $p<0.05$ was chosen as the threshold for statistical significance. In the case of multiple comparisons, Bonferroni's correction was applied.

References

1. Koike M, Shibata M, Tadakoshi M, Gotoh K, Komatsu M, Waguri S, et al. Inhibition of autophagy prevents hippocampal pyramidal neuron death after hypoxic-ischemic injury. Am J Pathol 2008; 172:454-69.
2. Puyal J, Vaslin A, Mottier V, Clarke PG. Postischemic treatment of neonatal cerebral ischemia should target autophagy. Ann Neurol 2009; 66:378-89.
3. Puyal J, Ginet V, Grishchuk Y, Truttmann AC, Clarke PG. Neuronal Autophagy as a Mediator of Life and Death: Contrasting Roles in Chronic Neurodegenerative and Acute Neural Disorders. Neuroscientist 2011.
4. Scarlatti F, Granata R, Meijer AJ, Codogno P. Does autophagy have a license to kill mammalian cells? Cell Death Differ 2009; 16:12-20.
5. Clarke PG. Developmental cell death: morphological diversity and multiple mechanisms. Anat Embryol (Berl) 1990; 181:195-213.
6. Blommaart EF, Krause U, Schellens JP, Vreeling-Sindelarova H, Meijer AJ. The phosphatidylinositol 3-kinase inhibitors wortmannin and LY294002 inhibit autophagy in isolated rat hepatocytes. Eur J Biochem 1997; 243:240-6.
7. Guillon-Munos A, van Bemmelen MX, Clarke PG. Role of phosphoinositide 3-kinase in the autophagic death of serum-deprived PC12 cells. Apoptosis 2005; 10:1031-41.
8. Xue L, Fletcher GC, Tolkovsky AM. Autophagy is activated by apoptotic signalling in sympathetic neurons: an alternative mechanism of death execution. Mol Cell Neurosci 1999; 14:180-98.
9. Chen Y, McMillan-Ward E, Kong J, Israels SJ, Gibson SB. Oxidative stress induces autophagic cell death independent of apoptosis in transformed and cancer cells. Cell Death Differ 2008; 15:171-82.
10. Denton D, Shravage B, Simin R, Mills K, Berry DL, Baehrecke EH, et al. Autophagy, not apoptosis, is essential for midgut cell death in Drosophila. Curr Biol 2009; 19:1741-6.
11. Shimizu S, Kanaseki T, Mizushima N, Mizuta T, Arakawa-Kobayashi S, Thompson CB, et al. Role of Bcl-2 family proteins in a non-apoptotic programmed cell death dependent on autophagy genes. Nat Cell Biol 2004; 6:1221-8.
12. Yu L, Alva A, Su H, Dutt P, Freundt E, Welsh S, et al. Regulation of an ATG7-beclin 1 program of autophagic cell death by caspase-8. Science 2004; 304:1500-2.
13. Eisenberg-Lerner A, Bialik S, Simon HU, Kimchi A. Life and death partners: apoptosis, autophagy and the cross-talk between them. Cell Death Differ 2009; 16:966-75.
14. Berry DL, Baehrecke EH. Growth arrest and autophagy are required for salivary gland cell degradation in Drosophila. Cell 2007; 131:1137-48.
15. Espert L, Codogno P, Biard-Piechaczyk M. What is the role of autophagy in HIV-1 infection? Autophagy 2008; 4:273-5.
16. Bialik S, Kimchi A. Autophagy and tumor suppression: recent advances in understanding the link between autophagic cell death pathways and tumor development. Adv Exp Med Biol 2008; 615:177-200.
17. Kroemer G, Levine B. Autophagic cell death: the story of a misnomer. Nat Rev Mol Cell Biol 2008; 9:1004-10.
18. Zaidi AU, McDonough JS, Klocke BJ, Latham CB, Korsmeyer SJ, Flavell RA, et al. Chloroquine-induced neuronal cell death is p53 and Bcl-2 family-dependent but caspase-independent. J Neuropathol Exp Neurol 2001; 60:937-45.

19. Scott RC, Juhasz G, Neufeld TP. Direct induction of autophagy by Atg1 inhibits cell growth and induces apoptotic cell death. Curr Biol 2007; 17:1-11.
20. Wang Y, Han R, Liang ZQ, Wu JC, Zhang XD, Gu ZL, et al. An autophagic mechanism is involved in apoptotic death of rat striatal neurons induced by the non-N-methyl-D-aspartate receptor agonist kainic acid. Autophagy 2008; 4:214-26.
21. Yousefi S, Perozzo R, Schmid I, Ziemiecki A, Schaffner T, Scapozza L, et al. Calpain-mediated cleavage of Atg5 switches autophagy to apoptosis. Nat Cell Biol 2006; 8:1124-32.
22. Maiuri MC, Zalckvar E, Kimchi A, Kroemer G. Self-eating and self-killing: crosstalk between autophagy and apoptosis. Nat Rev Mol Cell Biol 2007; 8:741-52.
23. Ginet V, Puyal J, Clarke PG, Truttmann AC. Enhancement of autophagic flux after neonatal cerebral hypoxia-ischemia and its region-specific relationship to apoptotic mechanisms. Am J Pathol 2009; 175:1962-74.
24. Puyal J, Clarke PGH. Targeting autophagy to prevent neonatal stroke damage. Autophagy 2009; 5:1060-1.
25. Beart PM, Lim ML, Chen B, Diwakarla S, Mercer LD, Cheung NS, et al. Hierarchical recruitment by AMPA but not staurosporine of pro-apoptotic mitochondrial signaling in cultured cortical neurons: evidence for caspase-dependent/independent cross-talk. J Neurochem 2007; 103:2408-27.
26. Koh JY, Wie MB, Gwag BJ, Sensi SL, Canzoniero LM, Demaro J, et al. Staurosporine-induced neuronal apoptosis. Exp Neurol 1995; 135:153-9.
27. Jantas D, Szymanska M, Budziszewska B, Lason W. An involvement of BDNF and PI3-K/Akt in the anti-apoptotic effect of memantine on staurosporine-evoked cell death in primary cortical neurons. Apoptosis 2009; 14:900-12.
28. Ichimura Y, Kumanomidou T, Sou YS, Mizushima T, Ezaki J, Ueno T, et al. Structural basis for sorting mechanism of p62 in selective autophagy. J Biol Chem 2008; 283:22847-57.
29. Valentim L, Laurence KM, Townsend PA, Carroll CJ, Soond S, Scarabelli TM, et al. Urocortin inhibits Beclin1-mediated autophagic cell death in cardiac myocytes exposed to ischaemia/reperfusion injury. J Mol Cell Cardiol 2006; 40:846-52.
30. Iwamaru A, Kondo Y, Iwado E, Aoki H, Fujiwara K, Yokoyama T, et al. Silencing mammalian target of rapamycin signaling by small interfering RNA enhances rapamycin-induced autophagy in malignant glioma cells. Oncogene 2007; 26:1840-51.
31. Hwang JY, Kim YH, Ahn YH, Wie MB, Koh JY. N-Methyl-D-aspartate receptor blockade induces neuronal apoptosis in cortical culture. Exp Neurol 1999; 159:124-30.
32. Nakajima M, Kashiwagi K, Ohta J, Furukawa S, Hayashi K, Kawashima T, et al. Etoposide induces programmed death in neurons cultured from the fetal rat central nervous system. Brain Res 1994; 641:350-2.
33. Takadera T, Matsuda I, Ohyashiki T. Apoptotic cell death and caspase-3 activation induced by N-methyl-D-aspartate receptor antagonists and their prevention by insulin-like growth factor I. J Neurochem 1999; 73:548-56.
34. Adamec E, Mohan PS, Cataldo AM, Vonsattel JP, Nixon RA. Up-regulation of the lysosomal system in experimental models of neuronal injury: implications for Alzheimer's disease. Neuroscience 2000; 100:663-75.
35. Maycotte P, Guemez-Gamboa A, Moran J. Apoptosis and autophagy in rat cerebellar granule neuron death: Role of reactive oxygen species. J Neurosci Res 2010; 88:73-85.

36. Wilson CA, Murphy DD, Giasson BI, Zhang B, Trojanowski JQ, Lee VM. Degradative organelles containing mislocalized alpha-and beta-synuclein proliferate in presenilin-1 null neurons. J Cell Biol 2004; 165:335-46.
37. Bampton ET, Goemans CG, Niranjan D, Mizushima N, Tolkovsky AM. The dynamics of autophagy visualized in live cells: from autophagosome formation to fusion with endo/lysosomes. Autophagy 2005; 1:23-36.
38. Finan PM, Thomas MJ. PI 3-kinase inhibition: a therapeutic target for respiratory disease. Biochem Soc Trans 2004; 32:378-82.
39. Wu YT, Tan HL, Shui G, Bauvy C, Huang Q, Wenk MR, et al. Dual role of 3-methyladenine in modulation of autophagy via different temporal patterns of inhibition on class I and III phosphoinositide 3-kinase. J Biol Chem; 285:10850-61.
40. Yee KS, Wilkinson S, James J, Ryan KM, Vousden KH. PUMA- and Bax-induced autophagy contributes to apoptosis. Cell Death Differ 2009; 16:1135-45.
41. Lee JS, Li Q, Lee JY, Lee SH, Jeong JH, Lee HR, et al. FLIP-mediated autophagy regulation in cell death control. Nat Cell Biol 2009; 11:1355-62.
42. Betin VM, Lane JD. Caspase cleavage of Atg4D stimulates GABARAP-L1 processing and triggers mitochondrial targeting and apoptosis. J Cell Sci 2009; 122:2554-66.
43. Boya P, Gonzalez-Polo RA, Casares N, Perfettini JL, Dessen P, Larochette N, et al. Inhibition of macroautophagy triggers apoptosis. Mol Cell Biol 2005; 25:1025-40.
44. Uchiyama Y. Autophagic cell death and its execution by lysosomal cathepsins. Arch Histol Cytol 2001; 64:233-46.
45. Pyo JO, Jang MH, Kwon YK, Lee HJ, Jun JI, Woo HN, et al. Essential roles of Atg5 and FADD in autophagic cell death: dissection of autophagic cell death into vacuole formation and cell death. J Biol Chem 2005; 280:20722-9.
46. Pattingre S, Espert L, Biard-Piechaczyk M, Codogno P. Regulation of macroautophagy by mTOR and Beclin 1 complexes. Biochimie 2008; 90:313-23.
47. Ciechomska IA, Goemans GC, Skepper JN, Tolkovsky AM. Bcl-2 complexed with Beclin-1 maintains full anti-apoptotic function. Oncogene 2009; 28:2128-41.
48. Takacs-Vellai K, Vellai T, Puoti A, Passannante M, Wicky C, Streit A, et al. Inactivation of the autophagy gene bec-1 triggers apoptotic cell death in C. elegans. Curr Biol 2005; 15:1513-7.
49. Fimia GM, Stoykova A, Romagnoli A, Giunta L, Di Bartolomeo S, Nardacci R, et al. Ambra1 regulates autophagy and development of the nervous system. Nature 2007; 447:1121-5.
50. Matsunaga K, Saitoh T, Tabata K, Omori H, Satoh T, Kurotori N, et al. Two Beclin 1-binding proteins, Atg14L and Rubicon, reciprocally regulate autophagy at different stages. Nat Cell Biol 2009; 11:385-96.
51. Takahashi Y, Meyerkord CL, Wang HG. Bif-1/endophilin B1: a candidate for crescent driving force in autophagy. Cell Death Differ 2009; 16:947-55.
52. Chu CT, Zhu J, Dagda R. Beclin 1-independent pathway of damage-induced mitophagy and autophagic stress: implications for neurodegeneration and cell death. Autophagy 2007; 3:663-6.
53. Zhu JH, Horbinski C, Guo F, Watkins S, Uchiyama Y, Chu CT. Regulation of autophagy by extracellular signal-regulated protein kinases during 1-methyl-4-phenylpyridinium-induced cell death. Am J Pathol 2007; 170:75-86.

54. Scarlatti F, Maffei R, Beau I, Ghidoni R, Codogno P. Non-canonical autophagy: an exception or an underestimated form of autophagy? Autophagy 2008; 4:1083-5.
55. Seo G, Kim SK, Byun YJ, Oh E, Jeong SW, Chae GT, et al. Hydrogen peroxide induces Beclin 1-independent autophagic cell death by suppressing the mTOR pathway via promoting the ubiquitination and degradation of Rheb in GSH-depleted RAW 264.7 cells. Free Radic Res 2011; 45:389-99.
56. McCoy F, Hurwitz J, McTavish N, Paul I, Barnes C, O'Hagan B, et al. Obatoclax induces Atg7-dependent autophagy independent of beclin-1 and BAX/BAK. Cell Death Dis 2010; 1:e108.
57. Tian S, Lin J, Jun Zhou J, Wang X, Li Y, Ren X, et al. Beclin 1-independent autophagy induced by a Bcl-XL/Bcl-2 targeting compound, Z18. Autophagy 2010; 6:1032-41.
58. Carloni S, Buonocore G, Balduini W. Protective role of autophagy in neonatal hypoxia-ischemia induced brain injury. Neurobiol Dis 2008; 32:329-39.
59. Diskin T, Tal-Or P, Erlich S, Mizrachy L, Alexandrovich A, Shohami E, et al. Closed head injury induces upregulation of Beclin 1 at the cortical site of injury. J Neurotrauma 2005; 22:750-62.
60. Rami A, Langhagen A, Steiger S. Focal cerebral ischemia induces upregulation of Beclin 1 and autophagy-like cell death. Neurobiol Dis 2008; 29:132-41.
61. Luo S, Rubinsztein DC. Apoptosis blocks Beclin 1-dependent autophagosome synthesis: an effect rescued by Bcl-xL. Cell Death Differ 2010; 17:268-77.
62. Deglon N, Tseng JL, Bensadoun JC, Zurn AD, Arsenijevic Y, Pereira de Almeida L, et al. Self-inactivating lentiviral vectors with enhanced transgene expression as potential gene transfer system in Parkinson's disease. Hum Gene Ther 2000; 11:179-90.
63. Perrin V, Regulier E, Abbas-Terki T, Hassig R, Brouillet E, Aebischer P, et al. Neuroprotection by Hsp104 and Hsp27 in lentiviral-based rat models of Huntington's disease. Mol Ther 2007; 15:903-11.
64. Vaslin A, Puyal J, Borsello T, Clarke PG. Excitotoxicity-related endocytosis in cortical neurons. J Neurochem 2007; 102:789-800.
65. Vaslin A, Puyal J, Clarke PG. Excitotoxicity-induced endocytosis confers drug targeting in cerebral ischemia. Ann Neurol 2009; 65:337-47.
66. Zucker B, Luthi-Carter R, Kama JA, Dunah AW, Stern EA, Fox JH, et al. Transcriptional dysregulation in striatal projection- and interneurons in a mouse model of Huntington's disease: neuronal selectivity and potential neuroprotective role of HAP1. Hum Mol Genet 2005; 14:179-89.

Figure Legends

Figure 1. Time-course of cell death, caspase-3 activation and autophagosome increase in staurosporine-treated cultured cortical neurons. (a) Left panel: quantification of pyknotic nuclei as a percentage of all nuclei, following exposure to 1μM staurosporine (STS), showing a progressive increase in neuronal death (ct: 10±2 %, 6h: 34±3 %, 12h: 84±3 %, 24h: 98±1 %; n≥12). Right hand panels: representative images of Hoechst-stained nuclei after 12h of DMSO (ct) or STS. Arrows indicate pyknotic nuclei. **(b)** Representative immunoblots for LC3 and cleaved caspase-3 and the corresponding quantification showing that STS treatment significantly increases cleaved caspase-3 (3h: 365±25 %, 6h: 675±78 %, 12h: 1014±77 %, 24h: 1499%±143 %) and LC3-II (3h: 260±19 %, 6h: 361±44 %, 12h: 380±22 %, 24h: 249±15 %) (n≥6). Values are expressed as a percentage of control. **(c)** Upper panels: Confocal images of LC3 immunolabeling (green) of two representative cultured cortical neurons at different time points following STS treatment. STS exposure induces a progressive increase in LC3-positive dots (green). Hoechst-stained nuclei are blue. Lower panel: quantification of the number of the LC3 positive dots per neuron, demonstrating a strong increase in the number of autophagosomes over the first 12h of STS treatment (ct: 5.9±1.4 %, 3h: 35±5.3 %, 6h: 40.4±2.6 %, 12h: 47.1±4.5 %; 24h: 17.9±2.2 %; n≥5, 20 neurons per experiment). Results are mean ± SEM**,** **p<0.01, ***p<0.001, versus control, Student's t-test. Bars = 20 μM.

Figure 2. Staurosporine treatment increases lysosomal activity and autophagic flux in cultured cortical neurons. (a) Enzymatic assay for acid phosphatase (AP), performed on protein extracts of cultured neurons (10μg) following exposure to 1μM staurosporine (STS),

indicating a moderate and transient increase in AP activity at 3h (125±6 %) and 6h (131±2 %). Values are expressed as a percentage of control (ct, 0.1% DMSO for 24h), **p<0.01, versus control; Student's t-test, n≥4. **(b)** Cytochemistry for AP 6h after STS treatment showing an increase in the number of large AP-positive puncta (right panels). Punctum areas have been quantified and classified in 3 size-groups: small (≤0.3μm^2), intermediate (>0.3 and ≤0.9μm^2) and large (>0.9 μm^2). STS treatment has substantially increased the percentage of large puncta (left panel). Values represent percentage of AP-positive puncta per size-group per neuron. **p<0.01 between DMSO and STS; Student's t-test, n≥15. **(c)** Cytochemistry for β-N-acetylhexosaminidase showing an increase in the size of β-N-acetylhexosaminidase-positive dots in STS-treated neurons (6h) compared to control. **(d)** Representative immunoblots for p62/SQSTM1 (upper panel) and the corresponding quantification (lower panel) showing that STS treatment significantly decreases p62 expression (3h: 75±5 %, 6h: 52±2 %, 12h: 30±1 %, 24h: 18%±1 %) (n≥4). Values are expressed as a percentage of control. **(e)** Representative immunoblots against LC3 and p62/SQSTM1 and the corresponding quantifications demonstrating that addition of bafilomycin A1 (BA1, 300 nM, 12h) to the cultures increases the level of LC3-II (BA1: 717±41 %) and p62/SQSTM1 (BA1: 169±18 %) relative to control (ct) indicating a blockage of autophagic degradation (n≥5). Combination of BA1 and STS treatment (6h after exposure to BA1) results in a greater increase in LC3-II than treatment with STS or BA1 alone (BA1+STS: 995±126 %; *p<0.05; Student's t-test) and mitigates the STS-induced degradation of p62/SQSTM1 (STS: 51±3 %, BA1+STS: 141±18 %, **p<0.01; Student's t-test) confirming that STS induces functional autophagy. Results are expressed as mean ± SEM. Bars = 20 μm. **(f)** Upper panels: confocal images of a representative cultured cortical neuron transfected with GFP RFP-LC3 DNA

construct at different time points following STS treatment. Lower panel: Quantification of the number of LC3-positives dots per neuron following STS treatment. Total LC3-positive dots per neuron (GFP^+ RFP^+ and GFP^- RFP^+ LC3-positives dots): ct: 10.3±1.9 %, 6h: 35.4±3.6 %, 12h: 71.3±4 %; early autophagosomes (GFP^+ RFP^+ LC3-positives dots): 6.3±1.4 %, 6h: 24.2±2.8 %, 12h: 47±3.1%; late autophagosomes (GFP^- RFP^+ LC3-positives dots): 4.5±1.4 %, 6h: 11.2±1.5 %, 12h: 24.3±1.8 %. Results are mean ± SEM**,** n=4 independent experiments (20 neurons per experiment). ***p<0.001, versus control, Student's t-test. Bars = 10 μM.

Figure 3. Combination of 3-methyladenine and Q-VD-OPH is highly protective against staurosporine neurotoxicity. (a) Quantification of pyknotic nuclei 12h after staurosporine (STS) exposure showing that pre-treatment with 3-methyladenine (3-MA, 10mM) or Q-VD-OPH (25μM) reduces STS-induced neuronal death, and combination of the two inhibitors affords greater neuroprotection than either treatment alone. Counts of pyknotic nuclei are expressed as a percentage of the total number of nuclei (ct, 0.1%DMSO) (n≥7). (STS: 82±2 %; STS+3-MA: 58±2 %; STS+Q-VD-OPH: 47±3 %; STS+3-MA+Q-VD-OPH: 28±2 %). **(b)** Representative Western blot and the corresponding quantification of cleaved caspase-3 12h after STS exposure, demonstrating that not only Q-VD-OPH but also 3-MA pre-treatments significantly decrease caspase-3 activation (STS: 1091±160 %; STS+3-MA: 717±92 %; STS+Q-VD-OPH: 108±31 %; STS+3-MA+Q-VD-OPH: 98±17 %). Values are expressed as a percentage of control (0.1% DMSO). Results are mean ± SEM, *p<0.05; **p<0.01, versus STS-treated, Student's t-test, n=3. **(c)** Quantification of AIF nuclear translocation following 6h of STS (right panel) (ct: 15±1 %; STS: 48±2 %, STS+3-MA: 19±1 %) and representative images of neurons immunostained for AIF (green) and Hoechst (blue) showing that pre-

treatment with 3-MA strongly reduces AIF nuclear translocation. Results are mean ± SEM**,** ***p<0.001, versus control, Student's t-test. n≥20. Bar = 20μm.

Figure 4. Knockdown of Atg5 reduces staurosporine-induced autophagy and apoptosis. **(a)** Q-RT-PCR assay for Atg5 in primary cortical neurons transduced with a lentiviral vector encoding shRNA targeted to Atg5 showing that Atg5 shRNA decreases Atg5 mRNA expression (47±0.6%) (***p<0.001, versus infection control, Student's t-test, n=5). **(b)** Confocal images of staurosporine (STS)-treated cortical neurons expressing sapphire-LC3 and immunolabeled with an antibody against GFP, showing that downregulation of Atg5 decreases strongly the presence of sapphire-LC3 positive dots. Bar = 10μm. Expression of **(c)** LC3-II (empty vector+STS: 308±38 %; shRNA Atg5+STS: 214±9 %) and **(d)** cleaved caspase-3 (empty vector+STS: 834±42 %; shRNA Atg5+STS: 444±49 %) are both significantly reduced in shRNA Atg5-treated neurons 12h after the application of STS as shown by representative Western blots and their corresponding quantifications. Values are expressed as a percentage of control (0.1% DMSO). Results are mean ± SEM, **p<0.01, shRNA Atg5 STS versus infection control STS, Student's t-test, n≥7. **(e)** Quantification of pyknotic nuclei 12h after STS exposure showing significantly reduced cell death in STS-treated neurons with Atg5 knockdown and near complete protection together with Q-VD-OPH (empty vector+STS: 88±1 %; shRNA Atg5+STS: 59±2 %; empty vector+STS+Q-VD-OPH: 60±2 %; shRNA Atg5+STS+Q-VD-OPH: 30±1 %). Results are mean ± SEM, ***p<0.001, Student's t-test, n≥6.

Figure 5. Knockdown of ATG7 inhibits staurosporine-induced autophagy and apoptosis. (a) Q-RT-PCR assay for Atg7 in primary cortical neurons transduced with lentiviral vectors encoding shRNAs targeted to Atg7 showing that shRNAs against Atg7 strongly decreases Atg7 mRNA relative to control infection (13±0.5 %) (n=5). **(b)** Representative Western blot and corresponding quantification showing the downregulation of Atg7 in neurons transduced with lentiviral shRNAs against Atg7 (47±2 %) compared to control neurons (n=9). **(c)** Confocal images of STS-treated cortical neurons expressing sapphire-LC3 and immunolabeled with an antibody against GFP demonstrating that downregulation of Atg7 decreases drastically the presence of sapphire-LC3 positive dots. Bar = 10μm. Expression of **(d)** LC3-II (empty vector: 293±22 %; shRNAs Atg7: 124±12 %) and **(e)** cleaved caspase-3 (empty vector: 565±27 %; shRNAs Atg7: 162±6 %) are both significantly reduced in neurons treated with Atg7 shRNAs 12h after the application of STS (1μM) as shown by representative Western blots and their quantifications (n≥6). Values are expressed as a percentage of control (0.1% DMSO). Results are mean ± SEM, ***p<0.001, Atg7 shRNAs versus infection control, Student's t-test. **(f)** Quantification of pyknotic nuclei 12h after STS exposure showing significant protection against STS with Atg7 knockdown and almost complete protection when Atg7 knockdown is combined with Q-VD-OPH (empty vector+STS: 88±1 %; shRNAs Atg7+STS: 48±2 %; empty vector+STS+Q-VD-OPH: 58±3 %; shRNAs Atg7+STS+Q-VD-OPH: 29±2 %). Results are mean ± SEM, ***p<0.001, Student's t-test, n≥6.

Figure 6. **Knockdown of Atg5 or Atg7 reduces nuclear accumulation of apoptosis inducing factor. (a)** Quantification of nuclear apoptosis inducing factor (AIF) staining

(average of nuclear fluorescence intensity/μm^2) reveals that AIF nuclear translocation stimulated by staurosporine (STS) is strongly reduced in neurons transduced with shRNAs against Atg5 or Atg7 compared to empty vector control (empty vector+STS: 55±3; shRNA Atg5+STS: 31±2; shRNAs Atg7+STS cortical: 26±3). Data are mean ± SEM. ***p<0.001, Student's t-test, n≥10. **(b)** Representative images of primary cortical neurons stained with anti-AIF antibody (green) and Hoechst (blue) infected with empty vector (left), shRNA Atg5 (middle) and shRNAs Atg7 (right) after 6h of STS (1μM) treatment showing a reduction of AIF nuclear translocation. Bars = 20μm.

Figure 7. Overexpression of Atg7 sensitizes neurons to staurosporine-induced apoptosis. **(a)** Representative Western blot and the corresponding quantification showing the upregulation of Atg7 expression in Atg7-myc-transduced neurons (n=7). **(b)** Confocal images of staurosporine (STS)-treated cortical neurons immunolabeled for LC3 showing an increase of LC3-positive dots in Atg7-myc-transduced neurons. Bar =10μm. **(c)** Representative Western blots and the corresponding quantifications demonstrating that overexpression of Atg7 increases the expression of both LC3-II (empty vector+STS: 248±12 %, Atg7-myc+STS: 362±44 %) and cleaved caspase-3 (empty vector+STS: 580±42 %, Atg7-myc+STS: 922±77 %) (n≥4). **(d)** Representative Western blots and the corresponding quantifications showing the effect of Atg7 overexpression on LC3-II levels with the addition of bafilomycin A1 (BA1) (empty vector+STS+BA1: 604±26 %, Atg7-myc+STS+BA1: 752±26 %) (n≥4). **(e)** Quantification of pyknotic nuclei 6h after STS exposure showing that Atg7 upregulation significantly increased cell death in normal and in STS-treated conditions (empty vector: 21±1 %; empty vector+STS: 40±2 %; Atg7-myc: 33±2 %; Atg7-myc+STS: 69±2 %) (n≥26). Results are mean ± SEM, *p<0.05, **p<0.01, ***p<0.001, Student's t-test.

Figure 8. Knockdown of Beclin1 does not affect staurosporine-induced autophagy but sensitizes neurons to apoptosis. (a) Representative Western blot and the corresponding quantification showing a downregulation of about 73% of Beclin-1 expression in neurons transduced with Beclin-1 shRNA compared to control neurons. (n≥5). **(b)** Confocal images of staurosporine (STS)-treated cortical neurons expressing sapphire-LC3 and immunolabeled with an antibody against GFP demonstrating that downregulation of Beclin1 has no effect on the formation of sapphire-LC3 positive dots. Bar = 10μm. **(c)** Expression of LC3-II (empty vector+STS: 301±13 %; shRNA Beclin1+STS: 322±19 %; n≥5) is not affected by downregulation of Beclin1 12h after STS exposure (1μM) as shown by representative Western blot and its quantifications but **(d)** is strongly decreased (empty vector: 368±66 %; shRNA Beclin1: 169±9 %, n=6) following rapamycin treatment (10 μg/ml, 24h). **(e)** Expression of cleaved-caspase-3 (empty vector: 84±7 %; empty vector+STS: 779±22 %; shRNA Beclin1: 342±33; shRNA Beclin1+STS: 2192±143 %) is dramatically increased by downregulation of Beclin1. Beclin1-enhanced caspase-3 activation following STS treatment is almost completely prevented by Q-VD-OPH (391±94 %) (n≥5). Values are expressed as a percentage of control (0.1% DMSO, uninfected) (mean ± SEM), ***$p<0.001$, Student's t-test. **(f)** Quantification of pyknotic nuclei 12h after STS exposure showing that Beclin1 knockdown significantly increases cell death in normal and in STS-treated conditions (empty vector: 23±1 %; empty vector+STS: 79±2 %; shRNA Beclin1: 56±2 %; shRNA Beclin1+STS: 100±0.4 %) (n≥26). Results are mean ± SEM, ***$p<0.001$, Student's t-test.

Figure 9. Knockdown of ATG7 inhibits apoptosis induced by etoposide or MK801. Representative Western blots and the corresponding quantifications showing that the levels

of cleaved caspase-3 and LC3-II are both increased by treatment with **(a)** MK801 (40μM) (cleaved caspase-3, 24h: 611±18 %, 48h: 874±61 %; LC3-II, 24h: 125±4 %, 48h: 175±9 %) or with **(b)** etoposide (10 μM) (cleaved caspase-3, 24h: 1096±142 %, 48h: 1025±140 %; LC3-II, 24h: 124±16 %, 48h: 143±2 %) (n≥4). Representative Western blots and the corresponding quantifications demonstrating that downregulation of Atg7 prevents the caspase-3 activation and LC3-II increase induced by 48h of **(c)** MK801 (cleaved caspase-3, empty vector: 939±38 %, shRNA Atg7: 126±10 %, LC3-II: empty vector: 281±19 %, shRNA Atg7: 80±5 %) or of **(d)** etoposide (cleaved caspase-3, empty vector: 1422±90 %, shRNA Atg7: 202±16 %; LC3-II, empty vector: 156±11 %, shRNA Atg7: 49±18 %) (n=4). Quantification of pyknotic nuclei 48h following (**e**) MK801 (empty vector: 44±1 %, shRNA Atg7 21±1 %) and (**f**) etoposide (empty vector: 57±1 %, shRNA Atg7 34±2 %) treatments shows that Atg7 downregulation provides strong neuroprotection (n≥7). Results are mean ± SEM, *p<0.05, **p<0.01, ***p<0.001, Student's t-test.

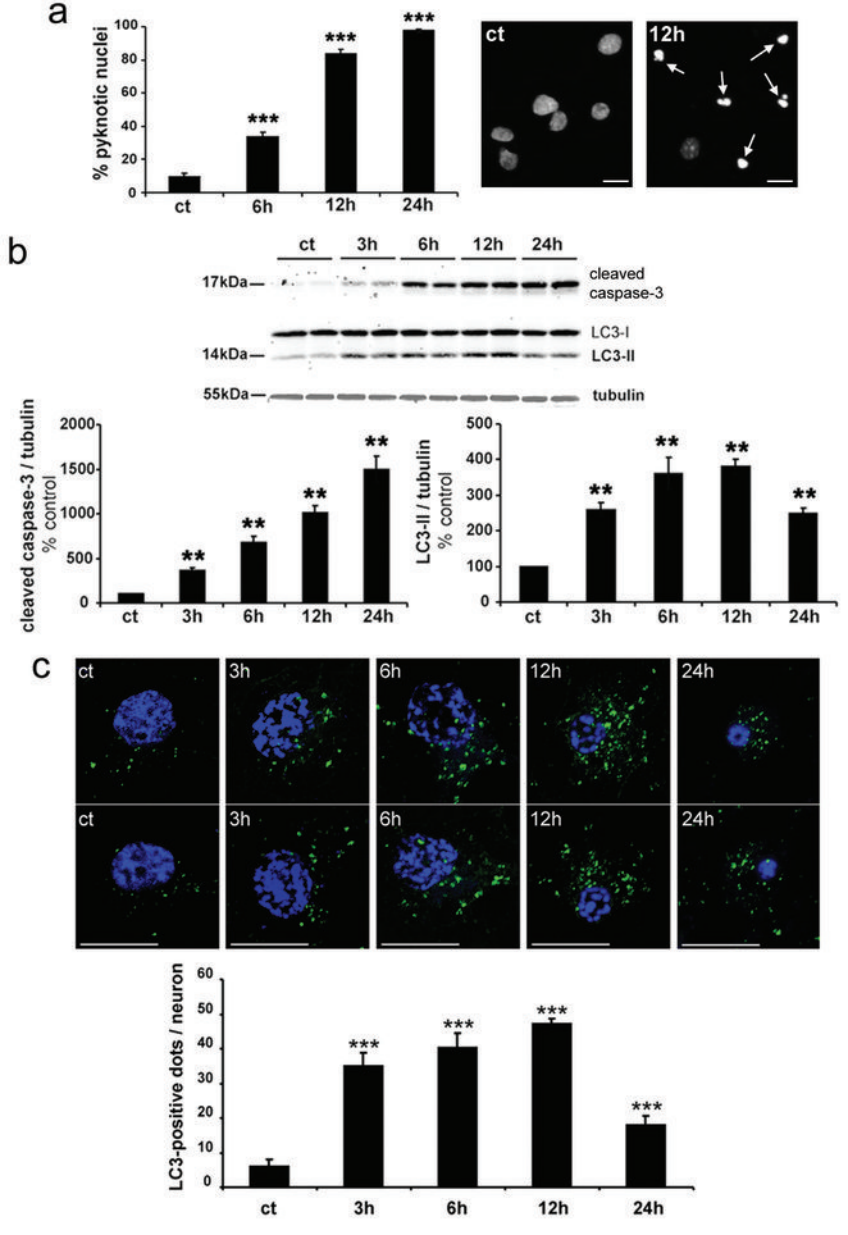
a
% pyknotic nuclei
100
80
60
40
20
0
***
***
***
ct
6h
12h
24h
ct
12h
b
ct
3h
6h
12h
24h
17kDa
cleaved caspase-3
LC3-I
14kDa
LC3-II
55kDa
tubulin
cleaved caspase-3 / tubulin % control
2000
1500
1000
500
0
**
**
**
**
ct
3h
6h
12h
24h
LC3-II / tubulin % control
500
400
300
200
100
0
**
**
**
**
ct
3h
6h
12h
24h
c
ct
3h
6h
12h
24h
ct
3h
6h
12h
24h
LC3-positive dots / neuron
60
50
40
30
20
10
0
***
***
***
***
ct
3h
6h
12h
24h

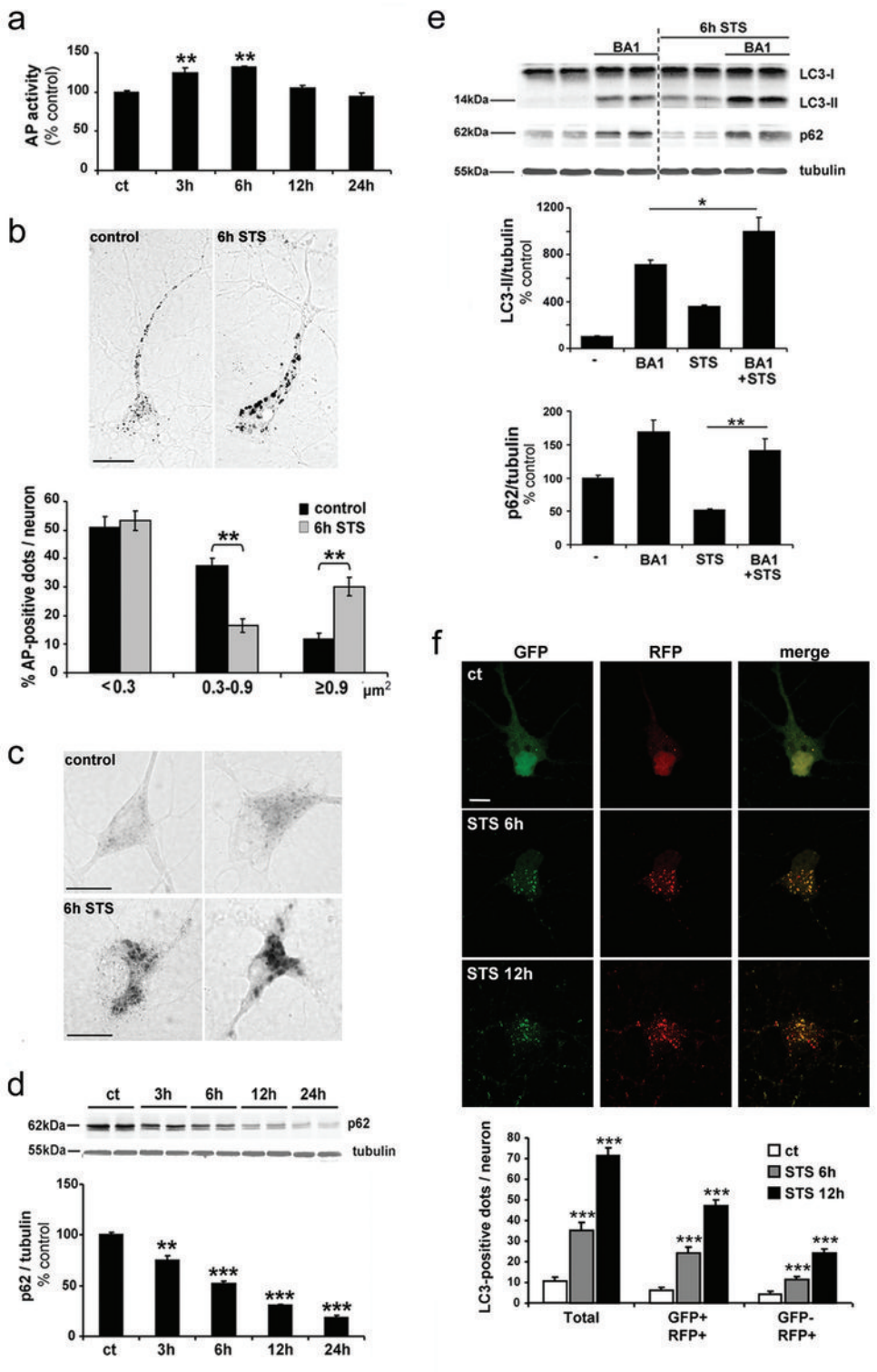
a
AP activity (% control)
150
100
50
0
**
**
ct
3h
6h
12h
24h
b
control
6h STS
% AP-positive dots / neuron
60
50
40
30
20
10
0
control
6h STS
**
**
<0.3
0.3-0.9
≥0.9
µm²
c
control
6h STS
d
ct
3h
6h
12h
24h
62kDa
p62
55kDa
tubulin
p62 / tubulin % control
150
100
50
0
**
***
***
***
ct
3h
6h
12h
24h
e
6h STS
BA1
BA1
LC3-I
14kDa
LC3-II
62kDa
p62
55kDa
tubulin
LC3-II/tubulin % control
1200
800
400
0
*
-
BA1
STS
BA1 +STS
p62/tubulin % control
200
150
100
50
0
**
-
BA1
STS
BA1 +STS
f
GFP
RFP
merge
ct
STS 6h
STS 12h
LC3-positive dots / neuron
80
70
60
50
40
30
20
10
0
***
***
***
***
***
***
ct
STS 6h
STS 12h
Total
GFP+ RFP+
GFP- RFP+

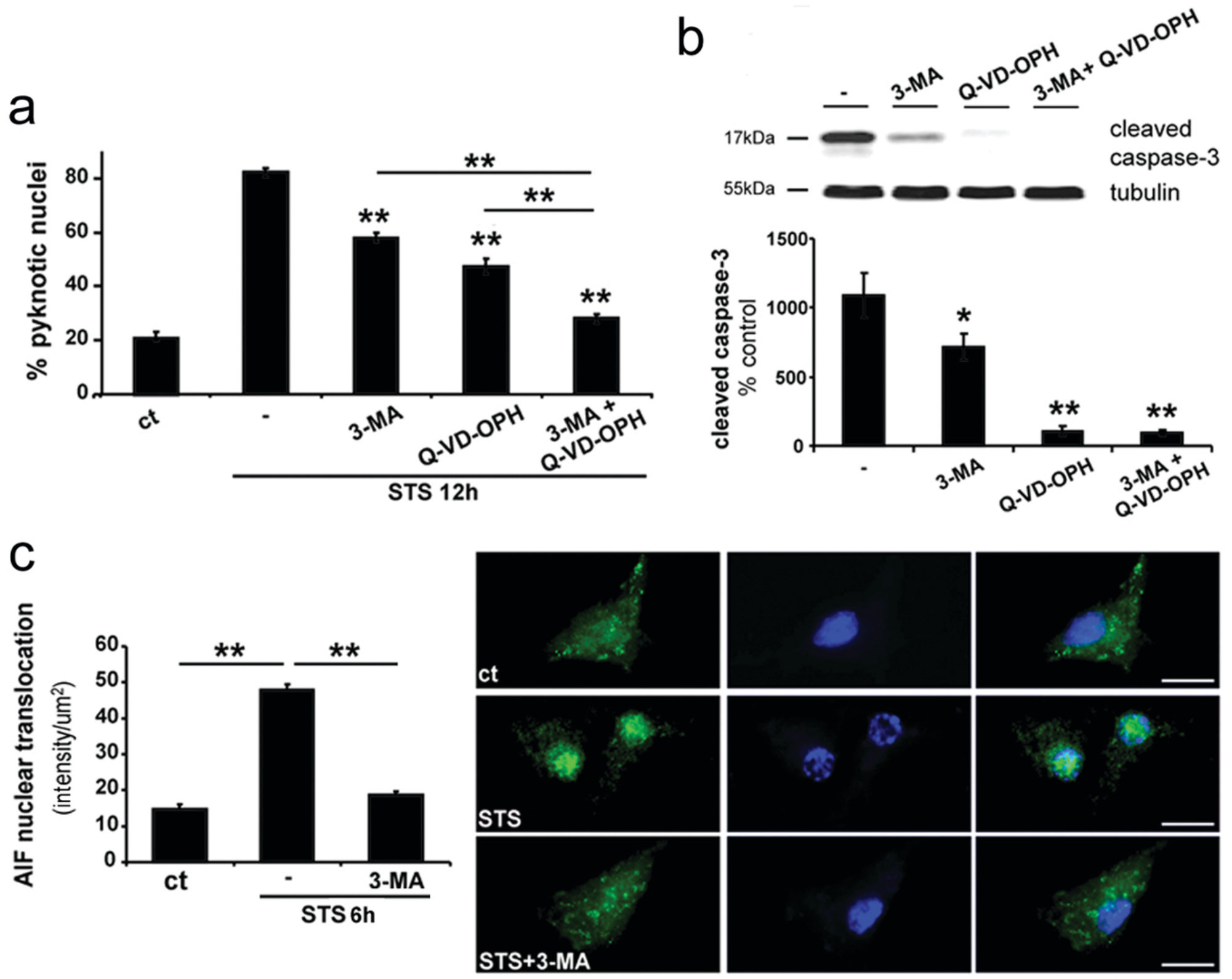
a
% pyknotic nuclei
0
20
40
60
80
**
**
**
**
ct
-
3-MA
Q-VD-OPH
3-MA + Q-VD-OPH
STS 12h
b
-
3-MA
Q-VD-OPH
3-MA+ Q-VD-OPH
17kDa
55kDa
cleaved caspase-3
tubulin
cleaved caspase-3 % control
0
500
1000
1500
*
**
**
-
3-MA
Q-VD-OPH
3-MA + Q-VD-OPH
c
AIF nuclear translocation (intensity/um2)
0
10
20
30
40
50
60
**
**
ct
-
3-MA
STS 6h
ct
STS
STS+3-MA

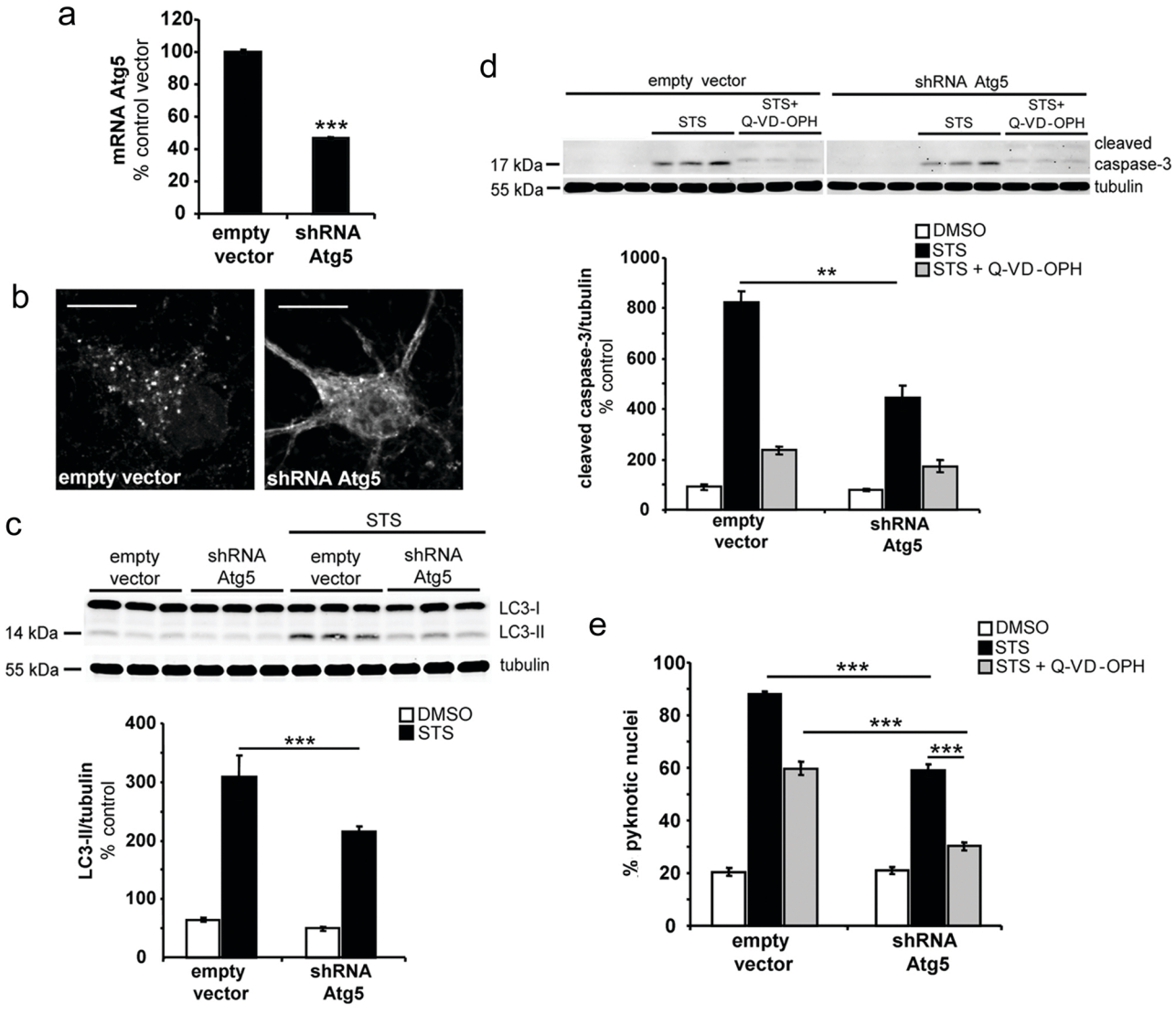
a
mRNA Atg5
% control vector
120
100
80
60
40
20
0
***
empty vector
shRNA Atg5
b
empty vector
shRNA Atg5
c
STS
empty vector
shRNA Atg5
empty vector
shRNA Atg5
LC3-I
LC3-II
14 kDa
55 kDa
tubulin
LC3-II/tubulin
% control
400
300
200
100
0
***
DMSO
STS
empty vector
shRNA Atg5
d
empty vector
shRNA Atg5
STS
STS+ Q-VD-OPH
STS
STS+ Q-VD-OPH
cleaved caspase-3
17 kDa
55 kDa
tubulin
DMSO
STS
STS + Q-VD-OPH
cleaved caspase-3/tubulin
% control
1000
800
600
400
200
0
**
empty vector
shRNA Atg5
e
DMSO
STS
STS + Q-VD-OPH
% pyknotic nuclei
100
80
60
40
20
0
***
***
***
empty vector
shRNA Atg5

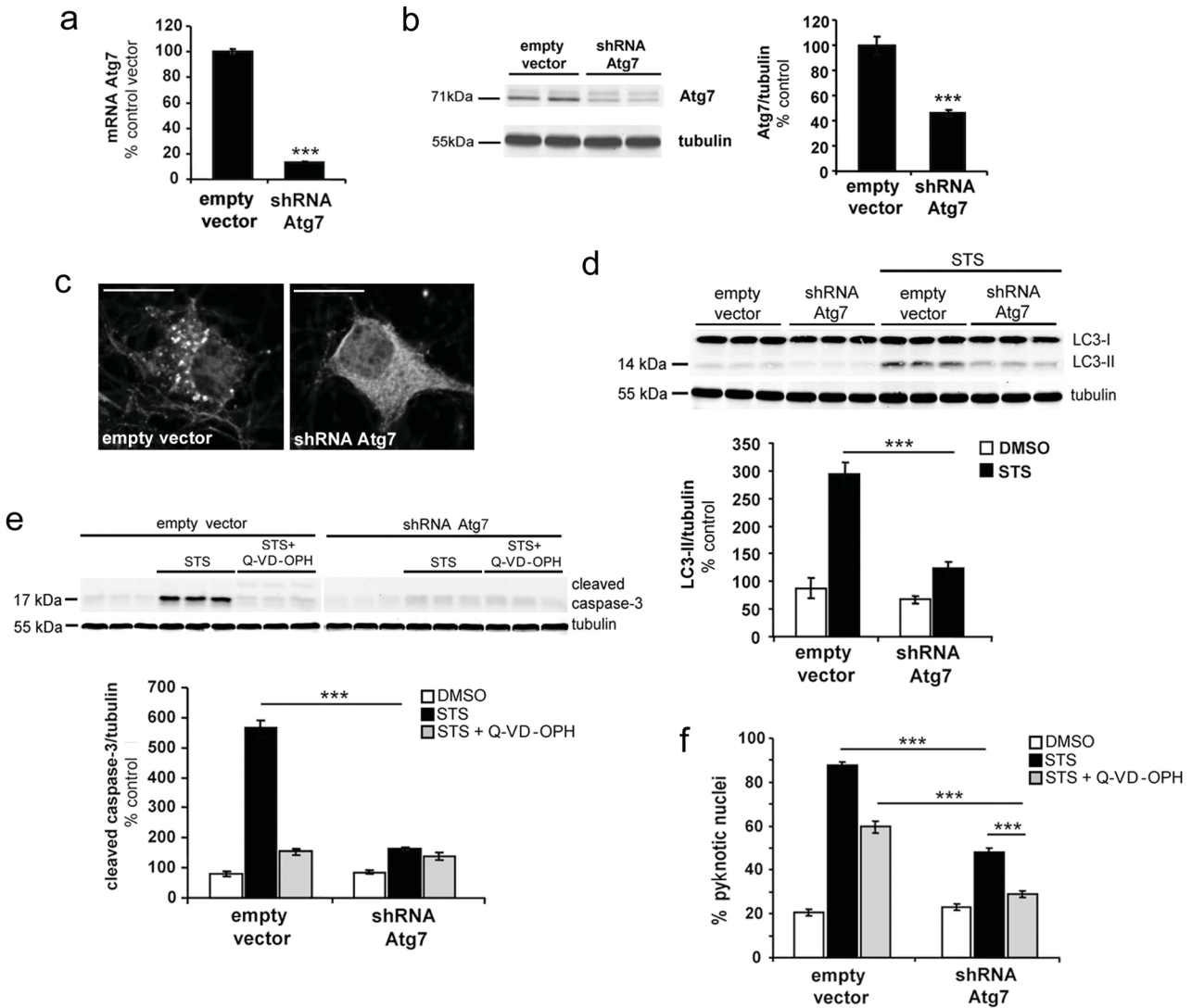
a
mRNA Atg7
% control vector
120
100
80
60
40
20
0
***
empty vector
shRNA Atg7
b
empty vector
shRNA Atg7
71kDa
Atg7
55kDa
tubulin
Atg7/tubulin
% control
120
100
80
60
40
20
0
***
empty vector
shRNA Atg7
c
empty vector
shRNA Atg7
d
STS
empty vector
shRNA Atg7
empty vector
shRNA Atg7
LC3-I
14 kDa
LC3-II
55 kDa
tubulin
LC3-II/tubulin
% control
350
300
250
200
150
100
50
0
***
DMSO
STS
empty vector
shRNA Atg7
e
empty vector
shRNA Atg7
STS
STS+ Q-VD-OPH
STS
STS+ Q-VD-OPH
17 kDa
cleaved caspase-3
55 kDa
tubulin
cleaved caspase-3/tubulin
% control
700
600
500
400
300
200
100
0
***
DMSO
STS
STS + Q-VD-OPH
empty vector
shRNA Atg7
f
% pyknotic nuclei
100
80
60
40
20
0
***
***
***
DMSO
STS
STS + Q-VD-OPH
empty vector
shRNA Atg7

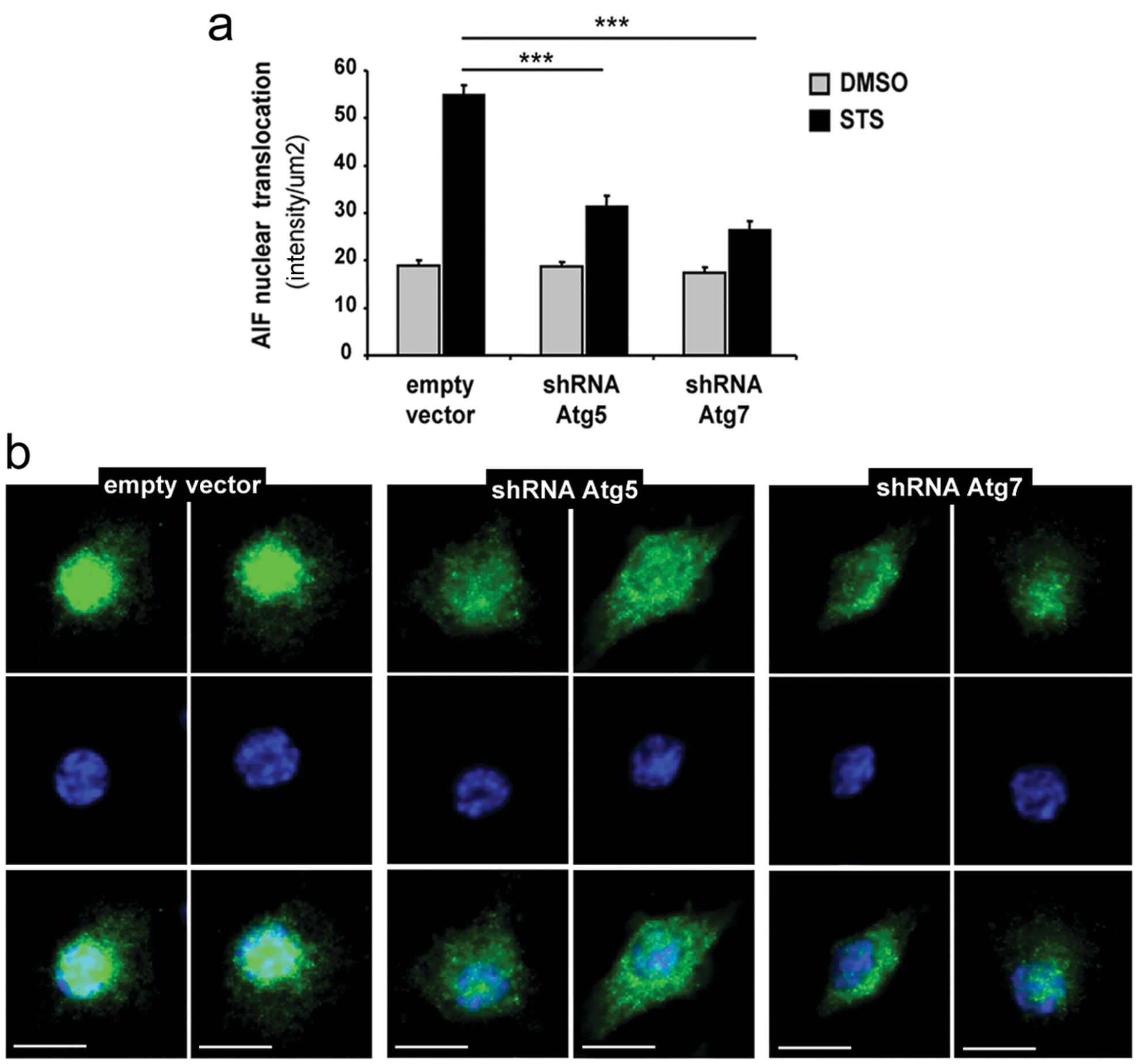
a
***
***
AIF nuclear translocation
(intensity/um2)
60
50
40
30
20
10
0
DMSO
STS
empty vector
shRNA Atg5
shRNA Atg7
b
empty vector
shRNA Atg5
shRNA Atg7

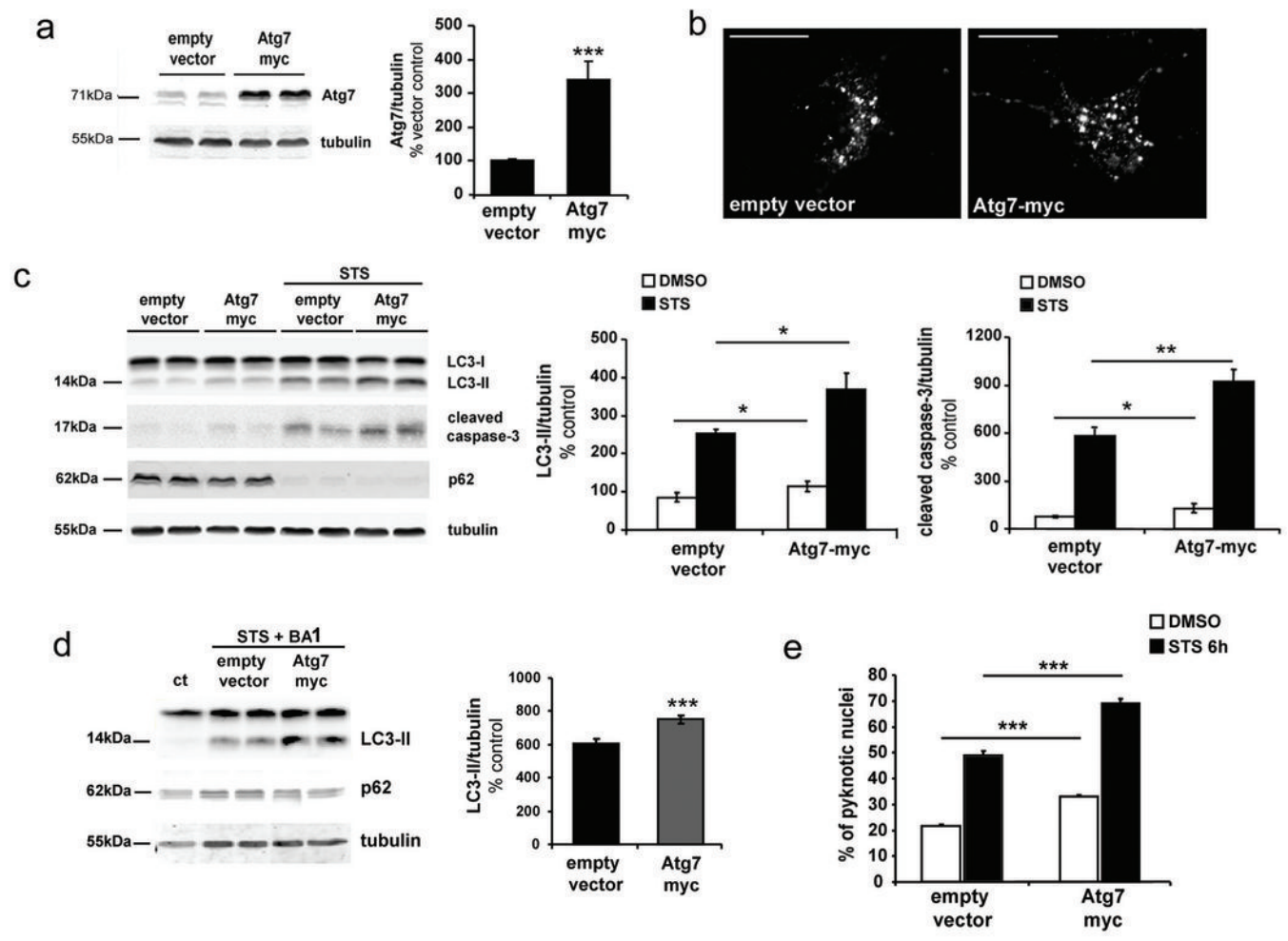
a
empty vector
Atg7 myc
71kDa
Atg7
55kDa
tubulin
Atg7/tubulin % vector control
500
400
300
200
100
0
***
empty vector
Atg7 myc
b
empty vector
Atg7-myc
c
STS
empty vector
Atg7 myc
empty vector
Atg7 myc
14kDa
LC3-I
LC3-II
17kDa
cleaved caspase-3
62kDa
p62
55kDa
tubulin
DMSO
STS
LC3-II/tubulin % control
500
400
300
200
100
0
*
*
empty vector
Atg7-myc
DMSO
STS
cleaved caspase-3/tubulin % control
1200
900
600
300
0
**
*
empty vector
Atg7-myc
d
STS + BA1
ct
empty vector
Atg7 myc
14kDa
LC3-II
62kDa
p62
55kDa
tubulin
LC3-II/tubulin % control
1000
800
600
400
200
0
***
empty vector
Atg7 myc
e
DMSO
STS 6h
% of pyknotic nuclei
80
70
60
50
40
30
20
10
0
***
***
empty vector
Atg7 myc

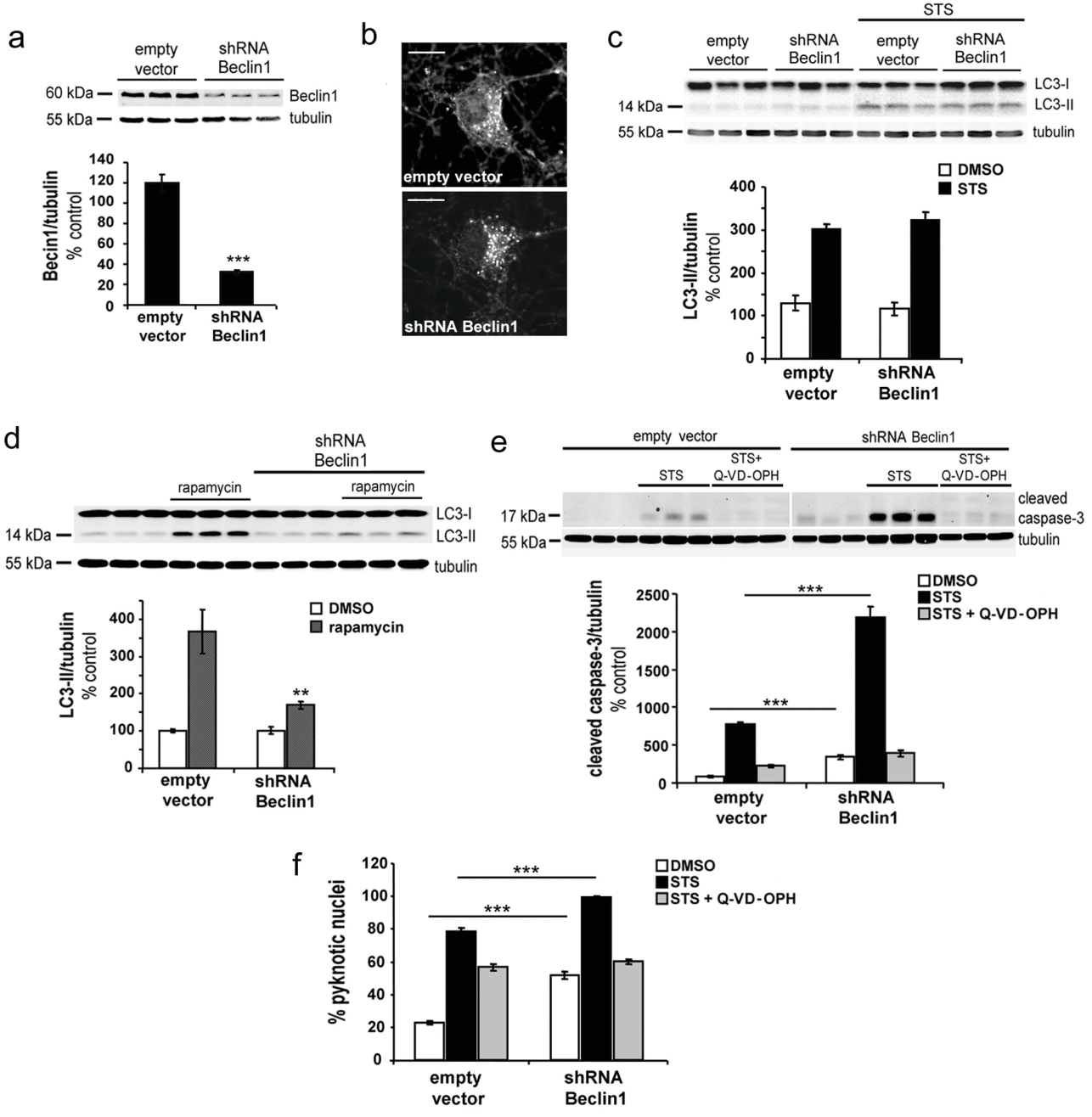
a
empty vector
shRNA Beclin1
60 kDa
55 kDa
Beclin1
tubulin
Becin1/tubulin % control
***
b
empty vector
shRNA Beclin1
c
STS
LC3-I
LC3-II
14 kDa
55 kDa
tubulin
DMSO
STS
LC3-II/tubulin % control
d
rapamycin
LC3-I
LC3-II
14 kDa
55 kDa
tubulin
DMSO
rapamycin
LC3-II/tubulin % control
**
e
STS
STS+ Q-VD-OPH
17 kDa
cleaved caspase-3
tubulin
DMSO
STS
STS + Q-VD-OPH
cleaved caspase-3/tubulin % control
***
f
% pyknotic nuclei
DMSO
STS
STS + Q-VD-OPH
***

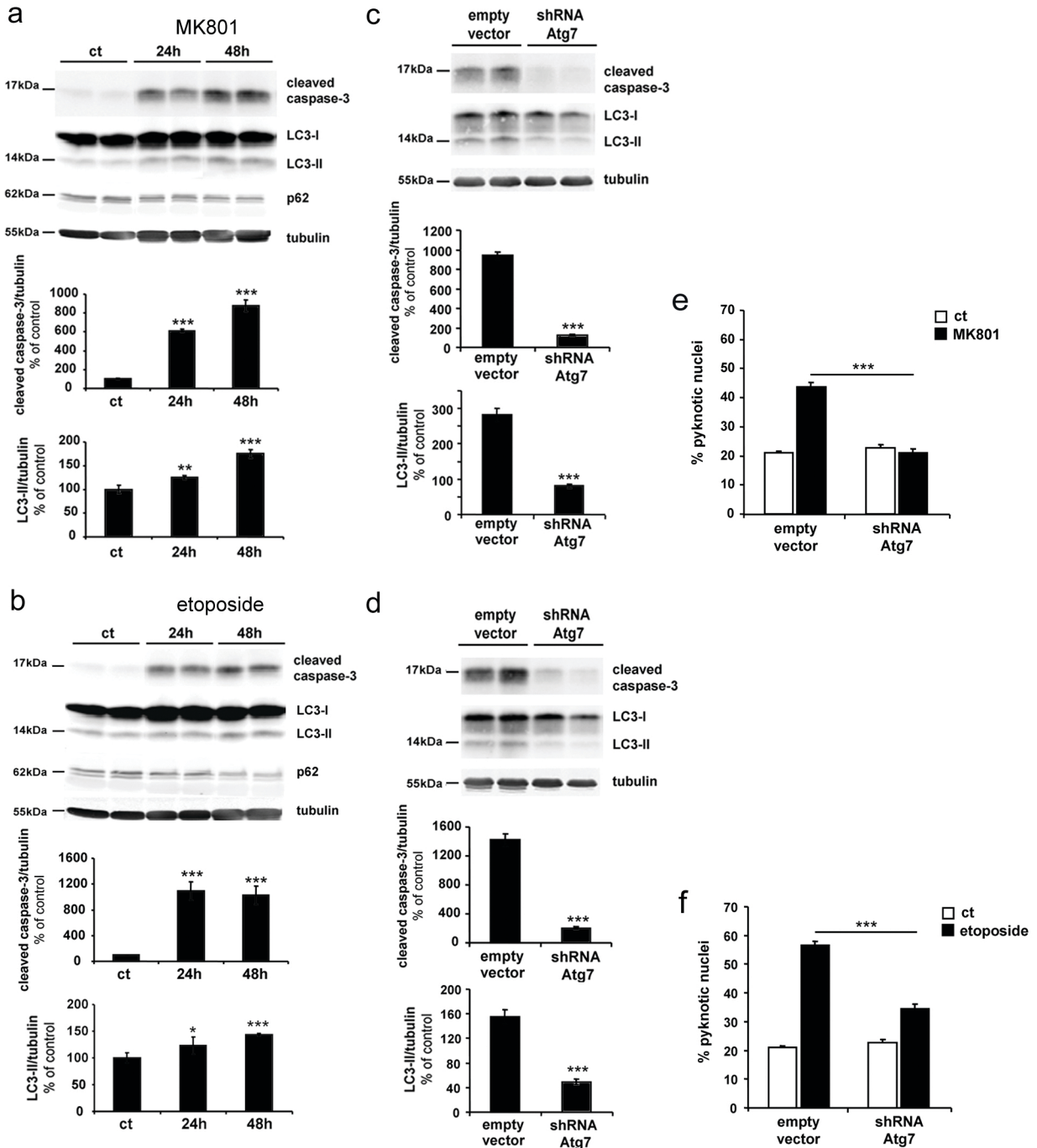
a
MK801
ct
24h
48h
17kDa
cleaved caspase-3
LC3-I
14kDa
LC3-II
62kDa
p62
55kDa
tubulin
cleaved caspase-3/tubulin % of control
LC3-II/tubulin % of control
b
etoposide
c
empty vector
shRNA Atg7
d
e
% pyknotic nuclei
ct
MK801
f
etoposide